© 2016. Published by The Company of Biologists Ltd | Development (2016) 143, 3969-3981 doi:10.1242/dev.139444

RESEARCH ARTICLE

Development of the neurons controlling fertility in humans: new insights from 3D imaging and transparent fetal brains

Filippo Casoni[1,2,*,‡,§], Samuel A. Malone[1,2,‡], Morgane Belle[3], Federico Luzzati[4,5], Francis Collier[6,7], Cecile Allet[1,2], Erik Hrabovszky[8], Sowmyalakshmi Rasika[9], Vincent Prevot[1,2,6], Alain Chédotal[3] and Paolo Giacobini[1,2,6,§]

ABSTRACT

Fertility in mammals is controlled by hypothalamic neurons that secrete gonadotropin-releasing hormone (GnRH). These neurons differentiate in the olfactory placodes during embryogenesis and migrate from the nose to the hypothalamus before birth. Information regarding this process in humans is sparse. Here, we adapted new tissue-clearing and whole-mount immunohistochemical techniques to entire human embryos/fetuses to meticulously study this system during the first trimester of gestation in the largest series of human fetuses examined to date. Combining these cutting-edge techniques with conventional immunohistochemistry, we provide the first chronological and quantitative analysis of GnRH neuron origins, differentiation and migration, as well as a 3D atlas of their distribution in the fetal brain. We reveal not only that the number of GnRH-immunoreactive neurons in humans is significantly higher than previously thought, but that GnRH cells migrate into several extrahypothalamic brain regions in addition to the hypothalamus. Their presence in these areas raises the possibility that GnRH has non-reproductive roles, creating new avenues for research on GnRH functions in cognitive, behavioral and physiological processes.

KEY WORDS: GnRH neurons, Human development, Fertility, Transparent brain, 3DISCO

INTRODUCTION

Reproduction and fertility in mammals depend on the function of a small population of cells – the gonadotropin-releasing hormone (GnRH) neurons. These neurons project to the hypothalamic median eminence and release GnRH into the pituitary portal blood circulation for delivery to the anterior pituitary, where it elicits the secretion of the gonadotropins, luteinizing hormone and follicle-stimulating hormone (Christian and Moenter, 2010). Failure of the GnRH system to develop or secrete properly is associated with clinical syndromes of reduced sexual competence or infertility (Boehm et al., 2015).

The development of the GnRH and olfactory systems are intimately entwined (Boehm et al., 2015). Indeed, during embryonic development GnRH neurons are born in the medial part of the nasal placode [the presumptive vomeronasal organ (VNO)] and enter the brain along a migratory route formed by the central trunk of the terminal (TN; nervus terminalis or cranial nerve 0), vomeronasal (VNN) and olfactory nerves (Schwanzel-Fukuda and Pfaff, 1989; Vilensky, 2014; Wirsig-Wiechmann and Oka, 2002; Wray et al., 1989). In humans, as in other vertebrates, the nasal placodes develop as thickenings of the ectoderm on the ventrolateral sides of the head around the fifth week of gestation (Muller and O'Rahilly, 2004). However, while the sequence and coordination of the events governing the differentiation and migration of GnRH neurons from the nose to the brain have been studied extensively in several species (Abraham et al., 2009; Bruneau et al., 2003; Murakami and Arai, 1994; Murakami et al., 1992; Palevitch et al., 2007; Quanbeck et al., 1997; Ronnekleiv and Resko, 1990; Schwanzel-Fukuda and Pfaff, 1989; Witkin et al., 2003; Wray et al., 1989), data in humans are scarce, relying mainly on scattered embryonic/fetal stages (Kim et al., 1999; Quinton et al., 1997; Schwanzel-Fukuda et al., 1989, 1996). To better understand the prenatal development and spatial organization of these neurons in humans, we combined immunohistochemistry with three-dimensional (3D) analysis of either reconstructed histological sections (Luzzati et al., 2011) or of optically cleared whole-mount embryos/fetuses (Belle et al., 2014; Ertürk et al., 2012; Renier et al., 2014).

Our results provide the first 3D atlas and cell counts of the developing GnRH neuronal system in humans during the first trimester of gestation. The breadth of analysis and level of detail made possible by these technologies reveal previously unprecedented target sites and routes of GnRH migration into the brain.

RESULTS

Formation of the olfactory placode and VNO

Most vertebrates possess two anatomically distinct olfactory systems: the main olfactory system, which is responsible for the detection of volatile odorants; and the vomeronasal system, which mediates the detection of pheromones, primarily non-volatile signals related to social and reproductive behavior (Dulac and Torello, 2003).

We first studied the sequential morphogenetic steps leading to the formation of the human olfactory/vomeronasal systems, the appearance of the first GnRH-expressing neurons and the initiation of the GnRH neuronal migratory process. In humans, the olfactory

[1]University of Lille, UMR-S 1172 - JPArc - Centre de Recherche Jean-Pierre AUBERT Neurosciences et Cancer, Lille 59000, France. [2]Inserm, UMR-S 1172, Laboratory of Development and Plasticity of the Neuroendocrine Brain, Lille 59000, France. [3]Sorbonne Université, UPMC Univ Paris 06, INSERM, CNRS, Institut de la Vision, Paris 75012, France. [4]Department of Life Sciences and Systems Biology (DBIOS), University of Turin, Turin 10123, Italy. [5]Neuroscience Institute Cavalieri Ottolenghi (NICO), Orbassano 10043, Italy. [6]FHU 1,000 Days for Health, University of Lille, School of Medicine, Lille 5900, France. [7]CHU Lille, Gynaecology Service - Hospital Jeanne de Flandre, Lille 59000, France. [8]Institute of Experimental Medicine, Laboratory of Endocrine Neurobiology, Budapest 1083, Hungary. [9]PROTECT, INSERM, Univ Paris Diderot, Sorbonne Paris Cité, Paris 75013, France. *Present address: Division of Neuroscience, San Raffaele Scientific Institute, Università Vita-Salute San Raffaele, Milan 20132, Italy.
‡These authors contributed equally to this work

§Authors for correspondence (filippo.casoni@unisr.it; paolo.giacobini@inserm.fr)

P.G., 0000-0002-3075-1441

Received 9 May 2016; Accepted 5 September 2016

Development (2016) 143, 3969-3981 doi:10.1242/dev.139444

placodes develop as thickenings of the ectoderm on the ventrolateral sides of the head around the fifth week of gestation (Muller and O'Rahilly, 2004). Although there is general agreement about the existence of a VNO in the human embryo (Smith and Bhatnagar, 2000), very little information is available about its development and molecular signature. Here, we first observed that the placodes invaginate at Carnegie stage (CS) 16 (~39th day of gestation) to form simple olfactory pits (Fig. 1A,B). An invagination of the medial olfactory placode gives rise to the presumptive vomeronasal organ (pVNO) (Fig. 1C,D). We analyzed the expression of the transcription factors AP-2α (TFAP2α) and PAX6, the graded expression of which defines the site of the VNO anlage in rodents (Forni et al., 2011). AP-2α immunoreactivity could be detected in the epidermis, dorsal and ventral craniofacial mesenchyme and a few ectodermal cells within the dorsal and ventral portions of the respiratory epithelium (Fig. 1A,B). In the nasal region, PAX6 expression was confined to the medial olfactory epithelium, with a decreasing gradient towards AP-2α-positive territories (Fig. 1A-C). We were able to identify symmetrical bean-shaped VNOs, located at the base of the nasal septum, in all embryos (CS 16-23, n=7; Figs 2 and 3) and fetuses [gestational weeks (GW) 9-12, n=8] analyzed. By CS 18, the VNO was closed and almost completely separated from the nasal cavity (Fig. 2A,B), except caudally, where it maintained contact with the olfactory epithelium throughout the first trimester of gestation (Fig. 2C, Fig. 3G).

Whether the VNO retains any proliferative capacity during embryogenesis in humans was unknown until now. At CS 20, numerous VNO cells expressed the proliferation marker Ki67 (MKI67) and high levels of the stem cell marker SOX2 (Fig. 2M,N). By contrast, they were negative for SOX10, a marker of olfactory ensheathing cells (a type of glial cell with myelinating capacity) and HuC/D (ELAVL3/4), a marker of immature neurons (Fig. 2M,N). These observations suggest that the embryonic VNO contains actively proliferating progenitors that could be the precursors of the neurons and olfactory ensheathing cells migrating into the telencephalon from the nasal region.

Ontogenesis of GnRH neurons and the 'migratory mass'

In rodents, early GnRH neurons migrate together with a heterogeneous coalescence of placode-derived and neural crest-derived migratory cells (Forni et al., 2011) and olfactory axons, collectively called the 'migratory mass' (MM) (Miller et al., 2010; Valverde et al., 1992). This cell migration precedes the targeting of olfactory sensory axons to the developing olfactory bulb (OB). The existence of a similar MM in the human embryo has not yet been described. We thus immunolabeled consecutive sagittal sections of a CS 16 embryo for GnRH and doublecortin (DCX) (Fig. 1D,E,G), a marker of immature migratory neurons (Gleeson et al., 1999). We identified a very small number (50 in total) of immature GnRH-expressing cells in the nasal mesenchyme, in the medial portion of the olfactory placode (Fig. 1C-E), adjacent to the basal lamina of the VNO, showing that the acquisition of cell identity occurs outside the VNO between GW 5 and 6. At this stage, we observed a mixed mass of immature GnRH neurons expressing DCX (Fig. 1F,G) or βIII-tubulin (Fig. 1H-J), migrating across the nasal mesenchyme towards the telencephalon. As in rodents (Miller et al., 2010), GnRH neurons in humans only represented a small proportion of the MM (Fig. 1G). Furthermore, these pioneer neurons of the MM expressed the delta/notch-like EGF repeat containing (DNER) (Fig. 1H-J), a transmembrane protein specifically localized in the dendrites and cell bodies of postmitotic neurons.

These data suggest that the morphogenetic programs defining the development of the olfactory and vomeronasal systems and the molecular signature of the GnRH migratory route are highly conserved across evolution (Eiraku et al., 2002; Miller et al., 2010).

Development of the VNN/TN and GnRH neuron migration

Neurons of the VNN and TN, which belong to the accessory olfactory system, develop simultaneously from the medial part of the nasal disc, together with GnRH neurons in mammals, including humans (Muller and O'Rahilly, 2004; Verney et al., 2002). The VNN and TN travel together across the nasal region (Brown, 1987), emerging from the vomeronasal epithelium and running medially from the olfactory epithelium towards the dorsal region of the OB. Their central entry, however, differs: it has previously been shown that the VNN reaches the dorsal region of the OB, namely the developing accessory olfactory bulb (AOB), which is responsible for coding pheromonal information after birth, whereas the TN projects both ventrally and dorsally within the forebrain, primarily to the septal, hypothalamic and limbic areas (Pearson, 1941a,b; Schwanzel-Fukuda and Silverman, 1980; Wirsig-Wiechmann and Oka, 2002).

Our immunohistochemical studies of CS 18 embryos revealed a mixed population of VNN and TN axons emerging from the VNO, traveling across the nasal septum, crossing the cribriform plate and projecting into the telencephalon (Fig. 2A). In other mammals, this axonal scaffold, which serves as a substrate for the migration of GnRH neurons, expresses transient axonal glycoprotein 1 (TAG-1; contactin 2) (Yoshida et al., 1995), the neuron-specific βIII-tubulin (Giacobini et al., 2008), as well as the neuronal type III intermediate filament protein peripherin (Wray et al., 1994). These markers are known to be expressed by a subset of developing olfactory, vomeronasal and terminal axons (Gorham et al., 1990, 1991) and to highlight the entire GnRH migratory scaffold from the olfactory pit to the medial septal area (Fueshko and Wray, 1994). Here, we show that peripherin (Fig. 2D) and TAG-1 (Fig. 2E) are both expressed along this scaffold of vomeronasal/terminal axons in CS 19 embryos. At CS 18-20 (~44 to 49 days of gestation), we observed GnRH-immunopositive neurons outside the VNO (Fig. 2A). These cells were migrating across the nasal septum along βIII-tubulin-positive (Fig. 2A) and TAG-1-positive (Fig. 2F,G) VNN/TN axon bundles, which emerged from the VNO to project to the developing OB. Of note, only a few days after their initial appearance, some GnRH neurons had already entered the telencephalon and could be seen in the OB, septum and ventral striatum (Fig. 2A). At CS 18, immunolabeling for the olfactory ensheathing cell marker SOX10 (Barraud et al., 2013; Forni et al., 2011; Miller et al., 2010), βIII-tubulin and GnRH revealed that olfactory ensheathing cells enwrapped VNN/TN axons (Fig. 2H). GnRH neurons intermingled with SOX10-positive cells and immature migratory neurons (βIII-tubulin positive) in the nasal mesenchyme, on their way from the VNO to the developing forebrain (Fig. 2I-L).

As mentioned above, in most terrestrial vertebrates the vomeronasal neurons project to the AOB. The presence of an accessory olfactory system has also been documented during fetal life in humans (Bossy, 1980). However, there is no evidence so far for a neuronal connection between the VNO and the AOB. We tested this possibility by performing immunohistochemistry for neuropilin 2 (NRP2) and GnRH on sagittal sections of GW 9 heads (n=2) containing both the VNO and the AOB (Fig. S1A-D). NRP2, the receptor for semaphorin 3F, is highly expressed by a subset of vomeronasal sensory neurons in rodent embryos and along

Development (2016) 143, 3969-3981 doi:10.1242/dev.139444

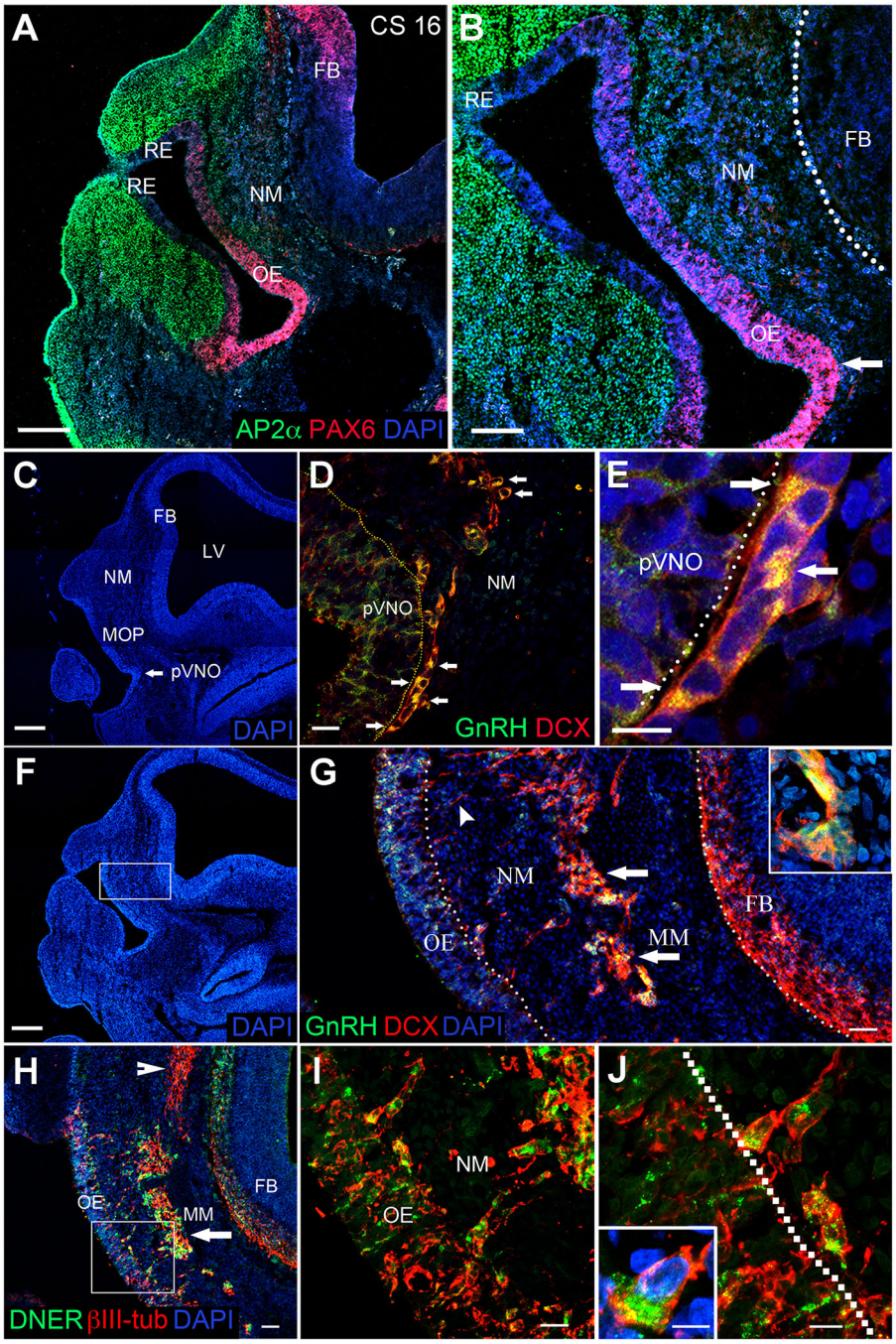

Fig. 1. Ontogenesis and molecular signature of human GnRH neurons at CS 16. (A,B) Representative AP-2α (green) and PAX6 (red) immunoreactivity in a sagittal section of a CS16 embryo head. AP-2α and PAX6 are expressed in opposite gradients in the nasal mesenchyme (NM) (AP-2α) and in the olfactory placodal epithelium (PAX6, arrow). (C) DAPI staining showing that in the olfactory placode an invagination of the medial olfactory placode (MOP) forms the presumptive vomeronasal organ (pVNO, arrow). (D) GnRH neurons (arrows) differentiate outside the pVNO and express DCX. (E) Early GnRH cells (arrows) are detected at the border between the NM and the epithelium of the pVNO. (F) Lateral sagittal section of a CS 16 embryo head stained with DAPI. (G) High magnification of the boxed area in F. Arrows point to cell clusters co-expressing GnRH and DCX. Arrowhead indicates a neurite process of a DCX-expressing migratory cell. Inset is a high-magnification view of migratory neurons expressing both GnRH and DCX. (H-J) The neuronal migratory mass (MM, arrows) expresses DCX. GnRH neurons coalescence with the MM. DNER$^+$ and βIII-tubulin$^+$ cells are detected in the medial NM forming the MM (H, arrow) and βIII-tubulin$^+$ cells are present dorsally towards the developing olfactory bulb (H, arrowhead). βIII-tubulin$^+$ neurons expressing DNER emerge from the olfactory epithelium (OE) (I) towards the coalescence of cells in the NM in a chain-like fashion. (J) High magnification of a βIII-tubulin$^+$ cell expressing DNER moving from the OE to the NM. The dotted line (J) delineates the boundary between the OE (left side) and the NM (right side). The inset (J) illustrates a migratory neuron, emerging from the OE, co-expressing DNER and βIII-tubulin. FB, forebrain; LV, lateral ventricle; RE, respiratory epithelium. Scale bars: A,C,F, 200 µm; B, 100 µm; D,I, 20 µm; E,J, 10 µm; inset in J, 5 µm; G,H, 50 µm.

vomeronasal axons innervating the AOB (Cariboni et al., 2007; Cloutier et al., 2002). Moreover, *Nrp2*$^{-/-}$ mice display a GnRH migratory defect followed by reduced fertility and hypogonadism, supporting the direct involvement of neuropilins and their ligands in the establishment of the GnRH neuroendocrine system (Cariboni et al., 2007).

We observed strong NRP2 expression in developing neurons of the VNO at GW 9, as well as along the VNN (Fig. S1B,C). GnRH neurons migrated in tight association with NRP2-positive fibers (Fig. S1C). Notably, analysis of the VNO target area revealed NRP2-expressing fibers in the AOB but not the main OB (Fig. S1D). These findings provide strong evidence for the anatomical connection between the human VNO and AOB.

High-resolution 3D imaging of the GnRH migratory pathway in transparent human embryos

3D imaging of solvent-cleared organs (3DISCO) is a solvent-based clearing method used to make the brain transparent (Ertürk et al., 2012; Ertürk and Bradke, 2013). This method has been combined with an immunolabeling protocol followed by light-sheet laser-scanning microscopy (LSM) to study neuronal connectivity in mouse embryos and postnatal brains (Belle et al., 2014; Ertürk et al., 2012). Here, we adapted this technique for the first time to intact human embryos and fetuses and gained excellent clearing of the specimens (Figs 3, 4, Movies 1-3). Whole-mount immunolabeling of a CS 19 human embryo (~48th day of gestation) for GnRH and peripherin followed by 3DISCO optical clearing and LSM provided

Development (2016) 143, 3969-3981 doi:10.1242/dev.139444

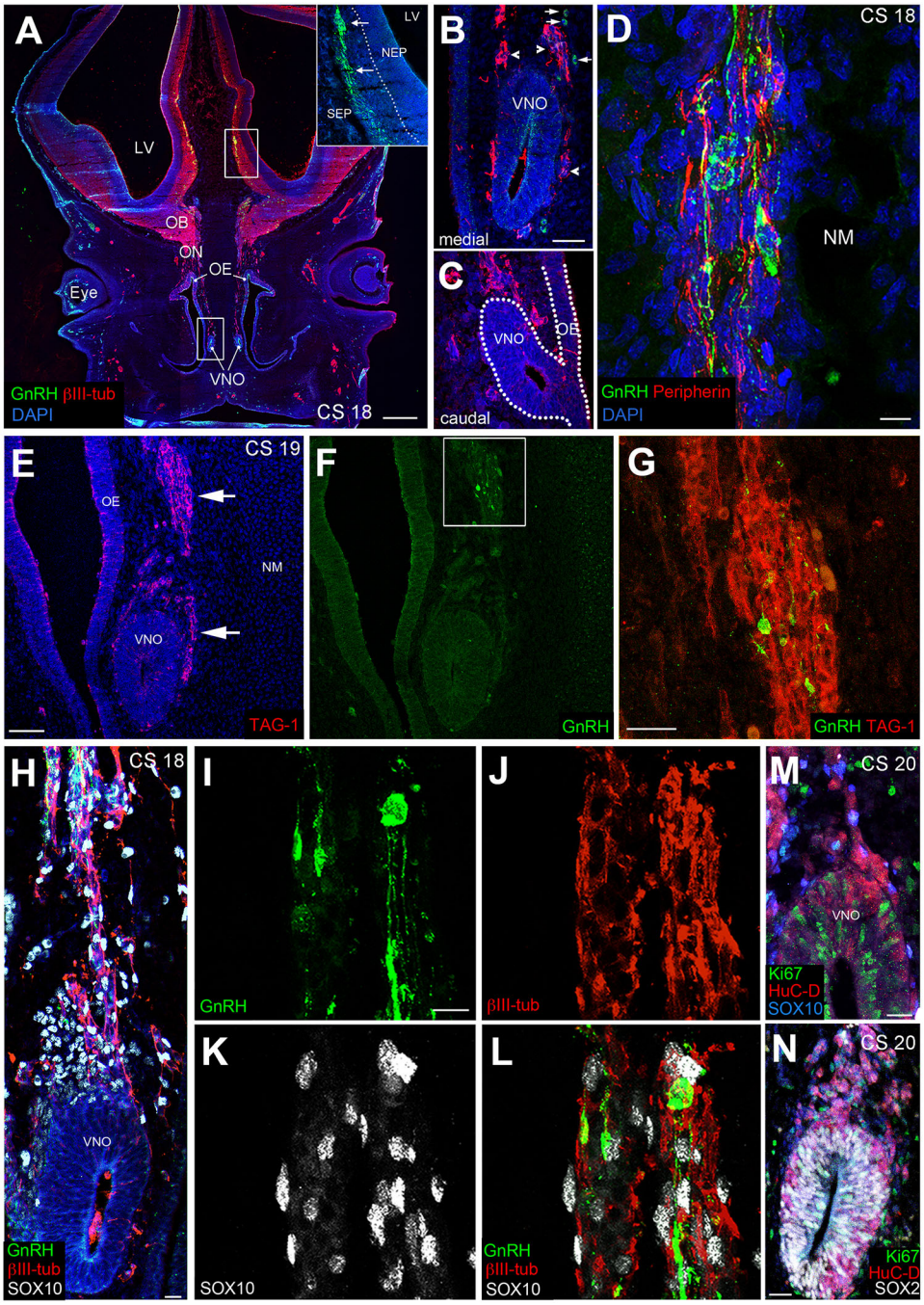

Fig. 2. Development of the VNO and related cellular components. (A-C) GnRH and βIII-tubulin expression in a coronal section of a CS 18 human embryo. (A) GnRH cells migrate along the vomeronasal nerve (VNN), which expresses βIII-tubulin (lower boxed region, as enlarged in B, arrows), in the olfactory bulb (OB), inside the brain at the level of the septum (white square; arrows in inset indicate GnRH neurons that reached the septum). (B) Magnification of the VNO and OE in A. Arrowheads indicate the VNN. (C) Caudally, the VNO is fused with the developing OE. (D) GnRH cells migrate along peripherin^{+} axons across the NM. (E-G) Confocal images for TAG-1^{+} (E, arrows) and GnRH^{+} (F) cells in a CS 19 embryo. (G) Higher magnification of the white box in F. TAG-1 is expressed along the VNN. (H-L) Triple immunolabeling showing expression of GnRH, βIII-tubulin and SOX10 in a coronal section of a VNO at CS 18. GnRH neurons (I) are intermingled in the NM with migratory neurons (βIII-tubulin^{+}, J) and ensheathing SOX10^{+} cells (K,L). (M,N) Expression of Ki67, HuC/D and SOX10 (M) or SOX2 (N) inside the VNO at CS 20. NEP, neuroepithelium; ON, olfactory nerve; SEP, septum; other abbreviations as Fig. 1. Scale bars: A, 500 µm; B,C, 50 µm; D,I-L, 10 µm; E,F, 60 µm; G,H,M,N, 20 µm.

high-resolution imaging of immunofluorescent signals (Fig. 3A-E, Movie 1). At this stage of embryonic development, a bilateral continuum of GnRH neurons migrated across the nasal region and started to enter the forebrain, directed towards the neocortex (NCX) and the septal areas (SEP) (Fig. 3B). The peripherin antibody allowed us to visualize motor and sensory fibers of the entire peripheral nervous system in human embryos, including cranial nerves, olfactory, vomeronasal and terminal fibers (Fig. 3C-E, Movie 1). The intracranial projections of the TN had already reached the medial septal area by this embryonic stage. Unexpectedly, a considerable subset of TN fibers sprouted dorsally and laterally to telencephalic regions corresponding to the NCX and the developing hippocampus. We found that GnRH neurons were consistently juxtaposed to the peripherin-positive VNN/TN while migrating from the nose into these telencephalic areas (Fig. 3C-E, Movie 1). We next optically sliced the immunolabeled head of the CS 19 embryo (Fig. 3F) and analyzed these digital coronal slices. The fact that GnRH neurons appear for the first time in the immediate vicinity of the VNO and nowhere else further establishes the VNO as their site of origin (Fig. 3F). These studies also confirm that the VNO maintains continuity with the olfactory epithelium in more caudal positions (Fig. 3F). We next performed whole-mount GnRH immunolabeling of a CS 21 human embryo (~53rd day of gestation) and documented the 3D distribution of GnRH neurons (Fig. 4A,B, Movie 2). At this stage, GnRH cells migrated within the brain in chain-like structures and proceeded dorsally and laterally towards

Development (2016) 143, 3969-3981 doi:10.1242/dev.139444

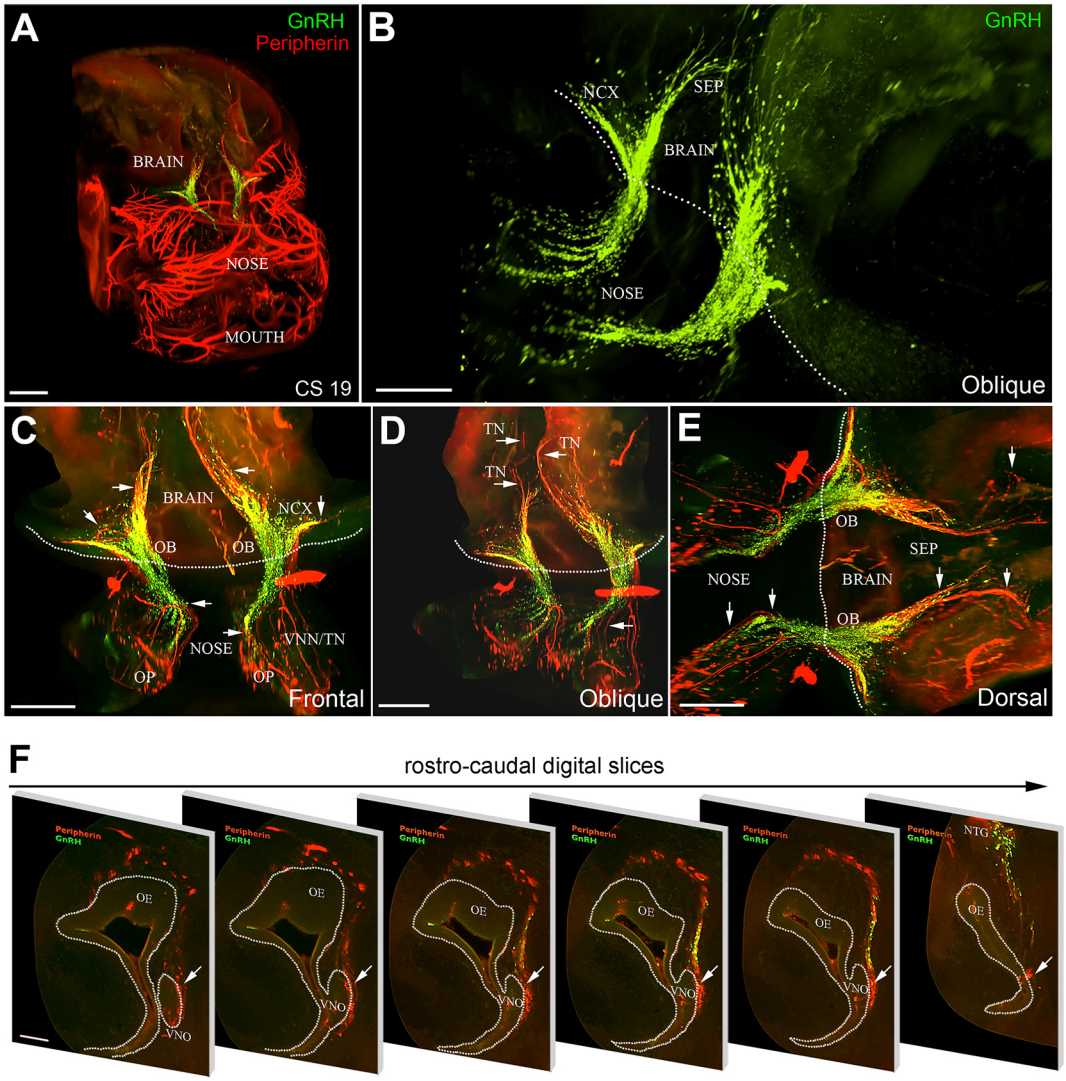

Fig. 3. Whole-mount immunolabeling and 3DISCO optical clearing of a CS 19 embryo. Representative image of a CS 19 human embryo after 3DISCO immunolabeling and optical clearing. (A-E) CS19 embryo labeled for GnRH and peripherin. (B-E) Different views of the entire transparent head depicting the GnRH migratory neurons (green) and the migratory scaffold (red, peripherin^{+}). Dotted lines define the boundaries between the nose and the brain. Arrows indicate the VNN/TN. (F) Rostrocaudal optical sections of the nasal region of the same embryo. GnRH neurons emerge from the VNO (arrows) and migrate along the VNN/TN. The VNO is separated from the OE rostrally but is fused with the OE caudally. NCX, neocortex; NTG, nervus terminalis ganglion; OP, olfactory placode; TN, terminal nerve; other abbreviations as previous figures. Scale bars: A, 800 µm; B, 200 µm; C-E, 300 µm; F, 100 µm.

the septum, OB and cortex (Fig. 4A,B, arrowheads). Moreover, some GnRH-positive cells formed a loop and started turning ventrally towards the developing hypothalamus (Fig. 4A,B).

A few days later, at GW 9, many GnRH neurons were still found in the nasal compartment in close association with TAG-1-immunoreactive VNN/TN axons. In addition, some GnRH cells had assumed an unexpected ring-like distribution, forming two symmetric circles around the developing OB (Fig. 4C,D, Movie 3). Inside the brain, GnRH neurons were no longer organized in continuous chains but were rather more widely spaced and scattered across multiple areas (Fig. 4E,F).

The distribution and number of GnRH neurons in the human fetal brain

In rodents, GnRH neurons migrate into the forebrain and appear to detach from the peripherin-positive terminals of VNN/TN fibers before entering the septal-preoptic area (Yoshida et al., 1995). In order to determine whether this was also the case in humans, coronal sections of a CS 23 embryo (~GW 8) were immunolabeled for peripherin and GnRH. Peripherin-positive fibers projected deeper than expected, to the mediobasal hypothalamus and developing median eminence (Fig. 5A). GnRH neurons were detectable in these regions, but always in tight apposition to peripherin-positive fibers right up to their target sites (Fig. 5A, inset). This suggests a fundamental difference between rodents and humans in the mode of migration of GnRH neurons during the last phase of their journey. Alternatively, VNN/TN axonal terminals might also persist in these areas in rodents, but no longer express peripherin.

At GW 9, in keeping with the identification of a dorsal/lateral branch of the TN in CS 19 embryos, GnRH neurons were distributed along two different migratory streams. The first, a ventral migratory pathway directed towards the presumptive hypothalamic regions (Fig. 5B, white arrow), has previously been documented in humans (Schwanzel-Fukuda et al., 1989, 1996). In addition, we provide evidence for an unexpected dorsal migratory pathway for GnRH

Development (2016) 143, 3969-3981 doi:10.1242/dev.139444

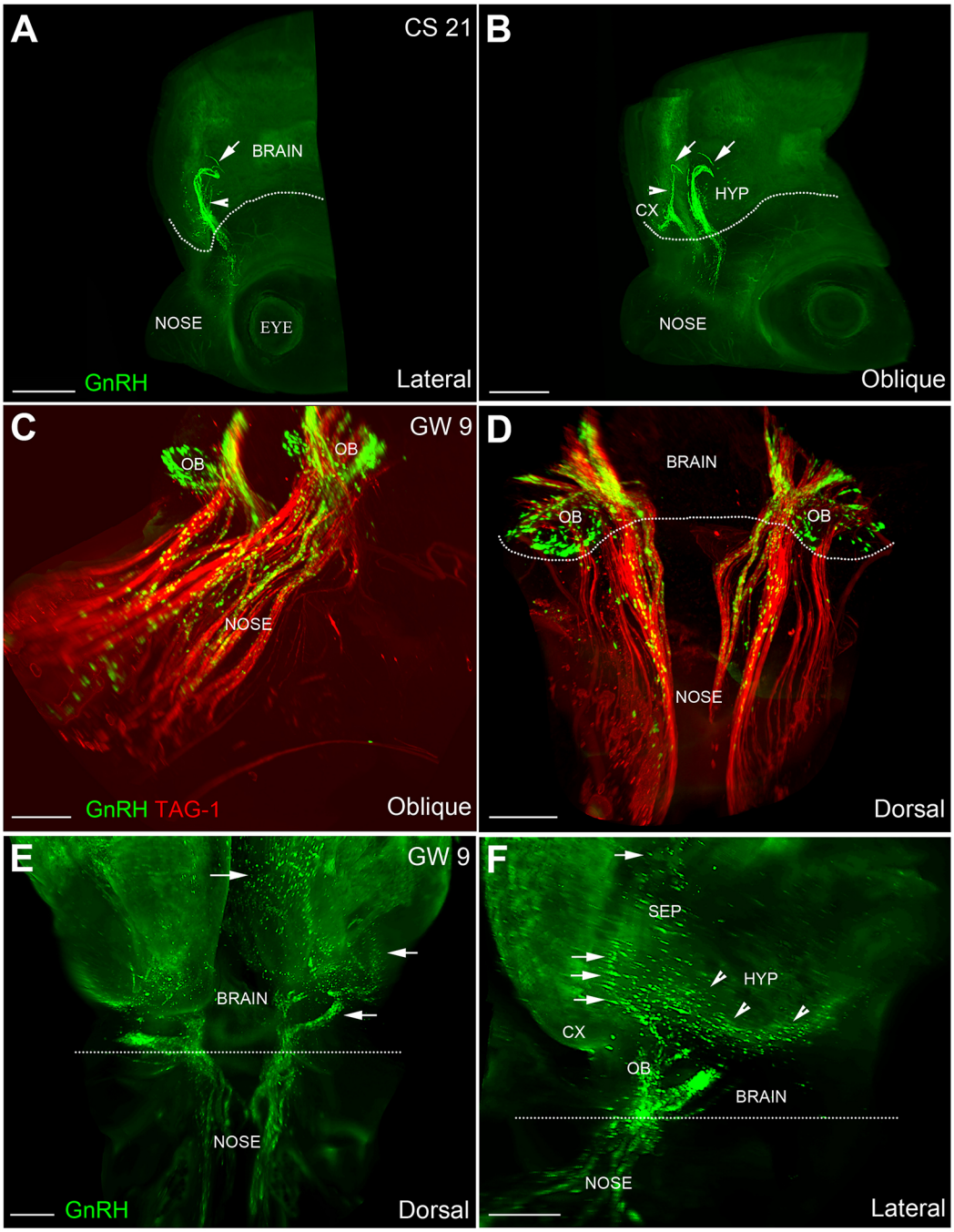

Fig. 4. Whole-mount immunolabeling and 3DISCO clearing of a CS 21 embryo and two GW 9 fetuses. (A,B) Lateral and oblique projections of the whole head of a CS 21 human embryo immunolabeled for GnRH. Chains of GnRH neurons enter the brain and progress either dorsally (arrows) or ventrally (arrowheads) toward the developing hypothalamus (HYP). (C,D) Whole-mount GnRH/TAG-1 immunolabeling of a GW 9 fetal nose. (E,F) Dorsal and lateral projections of a GW 9 head immunolabeled for GnRH. At this stage, GnRH neurons are distributed in several brain areas, including the HYP. CX, cortex; other abbreviations as previous figures. Scale bars: A,B, 500 µm; C,D, 200 µm; E, 300 µm; F, 400 µm.

neurons, directed towards pallial and subpallial telencephalic regions (Fig. 5B, red arrow).

Here, we counted for the first time the GnRH cells at different developmental stages between GW 5.5 (CS 16) and GW 12. At CS 16 (the earliest embryonic stage we had access to; n=1), we observed 50 GnRH neurons, all of which were restricted to the nasal region (Fig. 5C). Only a few days later [GW 6 (CS 17-18), n=3], the number of GnRH neurons had expanded to 7951±2000, indicating that (1) full GnRH neuronal differentiation occurs between 39 and 44 days of gestation and (2) GnRH neurons migrate rapidly during early embryogenesis (Fig. 5C). On average, ~10,000 immunoreactive GnRH neurons were detectable at four developmental stages spanning GW 6 to GW 12. This number is five times higher than previously estimated (Crowley et al., 2008; Tobet et al., 2001).

We did not observe any sex difference in the number of GnRH cells in GW 7-10 fetuses (n=4 males, mean GnRH cell number=11,123±2815; n=4 females, mean GnRH cell number=10,565±1693; t-test, P=0.8706). At each stage, we also quantified the relative distribution of GnRH cell bodies in three

Development (2016) 143, 3969-3981 doi:10.1242/dev.139444

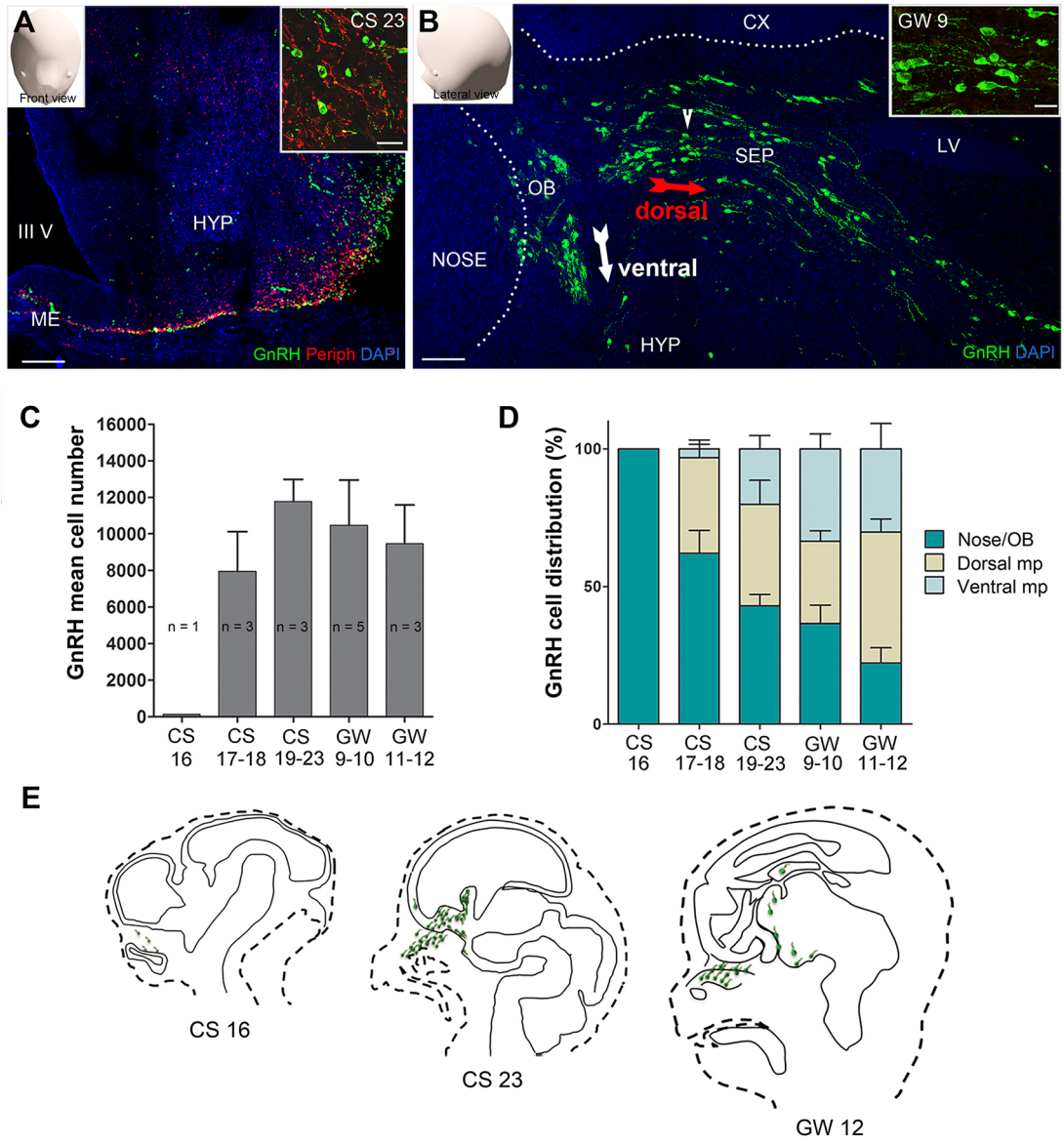

Fig. 5. Quantification of GnRH neurons during the first trimester of human gestation. (A) Representative coronal section of a GW 9 human fetal hypothalamus immunolabeled for GnRH (green) and peripherin (red). Peripherin^{+} fibers project to the basal hypothalamus and developing median eminence. Inset shows that GnRH neurons migrate to their final hypothalamic target areas in tight association with the peripherin^{+} fibers. (B) Representative sagittal section of a CS 23 fetal brain immunolabeled for GnRH. GnRH neurons enter the brain following a dorsal (red arrow) and a ventral (white arrow) migratory pathway. Inset shows migratory GnRH cells in the dorsal pathway at high magnification. Arrowhead indicates the region depicted in the inset. (C) Quantification of the mean total GnRH cell number during the first trimester of gestation in humans as a function of the developmental stages. (D) Distribution of GnRH cells expressed as a percentage of total cells calculated as a function of the developmental stages in three anatomical compartments: nose, dorsal and ventral migratory pathway (mp). (E) Schematic representation of GnRH migration during the first trimester of gestation in humans. Values are mean±s.e.m. ME, median eminence; III V, third ventricle; other abbreviations as previous figures. Scale bars: A, 100 µm; inset in A, 20 µm; B, 50 µm; inset in B, 10 µm.

areas: the nose/OB, and the ventral and dorsal migratory streams (Fig. 5D). At CS 16, GnRH immunoreactivity was restricted to the nose. At CS 17-18, ∼60% of the cells were migrating within the nose, 36% had entered the brain along the dorsal migratory stream and 4% had started to turn ventrally towards the basal forebrain. During subsequent stages (CS 19 to GW 12, n=11; Fig. 5D,E), the number of cells in the nose progressively decreased, with a concomitant increase in cells in the dorsal and ventral migratory pathways. At the latest time point analyzed (GW 11-12, n=3), only 23% of GnRH neurons were located in the more rostral regions (nose/OB).

To understand in greater detail the anatomical distribution of GnRH neurons in human fetal brains, we performed 3D reconstruction analysis of serial sections at this fetal stage (GW 9, n=2; Fig. 6A, Movie 4). Our analysis confirmed that GnRH neurons migrated into the brain along two main migratory pathways, including the newly identified dorsal pathway. The latter pathway comprised two components: (1) one medial, reaching the septum/diagonal band of Broca, indusium griseum/presumptive hippocampus and rostromedial neocortex; and (2) one lateral, reaching the ventral striatum, piriform cortex and amygdala (Fig. 6A).

An anatomical atlas of developing human GnRH cells is currently unavailable. To generate a detailed distribution map of GnRH neurons in GW 12 fetuses (the latest developmental stage available for these studies), we immunolabeled serial coronal sections of GW

Development (2016) 143, 3969-3981 doi:10.1242/dev.139444

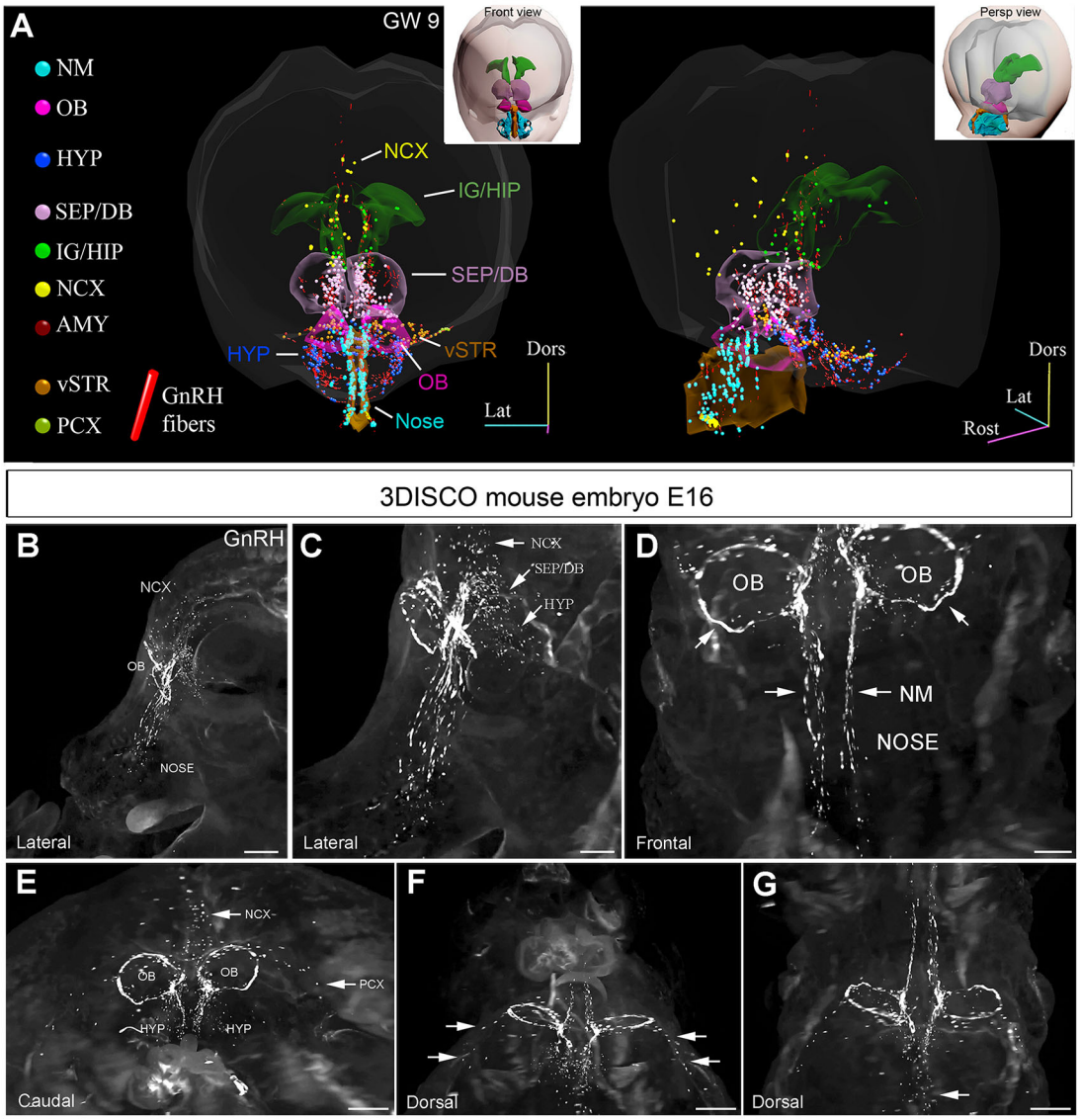

Fig. 6. GnRH neurons migrate following a dorsal and a ventral migratory pathway in both human and mouse fetuses. (A) Front (left) and perspective (right) views of a 3D atlas of the distribution of GnRH neuronal cell bodies and fibers in a GW 9 human embryo. Each cell is represented by a sphere (100 µm in diameter) colored according to its location (legend on the left). Transparent contours of the NM, OB, septum/diagonal band of Broca (SEP/DB) and indusium griseum/hippocampus (IG/HIP) are also shown for reference. In the inset, the position of these contours, together with the nasal turbinates (cyan), is shown. (B-G) Lateral (B,C), frontal (D), caudal (E) and dorsal (F,G) projections of the whole head of an E16.5 mouse embryo immunolabeled for GnRH and cleared using 3DISCO. GnRH neurons are found in the NCX, SEP/DB and HYP (arrows in C), around the OB (arrows in D), in the NCX and piriform cortex (PCX; arrows in E and F) and in deep brain areas corresponding to the fornix and developing hippocampus (arrow in G). AMY, amygdala; vSTR, central striatum; other abbreviations as previous figures. Scale bars: B, 400 µm; C, 200 µm; D, 180 µm; E-G, 600 µm.

12 heads and performed a 3D reconstruction of GnRH cell bodies and fibers (n=2; Fig. S2A,B, Movie 5). This experiment revealed a surprisingly wide distribution of GnRH cell bodies and fibers in the hypothalamus (Fig. S2A-D) as well as several extrahypothalamic areas, including the OB, cerebral cortex, hippocampus, piriform cortex, amygdala and habenula (Fig. S2A,B,E).

Two forms of GnRH are present in the human brain. Mammalian GnRH (GNRH1) regulates the reproductive axis (Guillemin, 1967), whereas the function of GNRH2, originally isolated from the chicken hypothalamus (cGnRH-2) (Miyamoto et al., 1984), is largely unknown. In order to verify whether the GnRH-immunoreactive neurons that we found in the human fetal brain contain the GNRH1 form, each antiserum was preabsorbed for 24 h at 4°C with the GNRH1 peptide (GeneCust, Luxemburg) at 5 µg/ml (Fig. S3A-D). High sequence homology between the GNRH1 and GNRH2 decapeptides (only three amino acid substitutions) could allow GNRH1 antibodies to cross-react with GNRH2. Therefore, we performed fluorescent *in situ* hybridization (FISH) experiments using a cRNA probe directed against *GNRH1* mRNA, where lack of significant nucleotide sequence homology would rule out any cross-reactivity of the *GNRH1* probe with *GNRH2* mRNA. These experiments confirmed that the fetal GnRH neurons express *GNRH1* (Fig. S3E,F). This was further confirmed by performing dual-fluorescent labeling experiments on a GW 10 and a GW 12 fetus (Fig. S4), combining the use of an anti-GnRH (guinea pig) antibody, which can potentially bind all GnRH forms, with a mouse polyclonal antibody directed against a human GnRH-associated peptide 1 (GAP1) sequence (Skrapits et al., 2015), which is specific

Development (2016) 143, 3969-3981 doi:10.1242/dev.139444

for the GNRH1. These experiments revealed that all GnRH-immunoreactive neurons that we found in the human fetal brain contain the GNRH1 form (Fig. S4A-H).

Confirmation of novel human findings in the mouse embryo

In light of the various novel observations made above regarding GnRH neuronal migration and distribution in humans, we addressed the possibility that some of these features might have been previously overlooked in rodents due to the scattered GnRH population and the limitations of conventional 2D histology. Using 3DISCO technology coupled with LSM, we performed a detailed topographical analysis of individual GnRH-immunoreactive neurons scattered over large brain areas of an E16 whole mouse embryo (Fig. 6B-G, Movie 6). This analysis confirmed the presence of a dorsal tract of migratory GnRH neurons, comprising two telencephalic cell populations oriented dorsally and laterally (Fig. 6B-D, Movie 6), in addition to the well-known ventral pathway. Our analysis also revealed a small GnRH neuronal population in pallial and subpallial regions (Fig. 6C,F,G). Mimicking our observations in human fetuses (Fig. 4C,D), GnRH neurons in mouse embryos formed a peculiar ring of cells surrounding the trunk of the OB (Fig. 6D). We further investigated whether GnRH neurons were still present in the mouse OB postnatally or if they were lost during development (Fig. 7, Movie 7). In whole-mount GnRH-immunolabeled adult mouse brain hemispheres (n=2, 4-month-old males; Fig. 7A-E, Movie 7), GnRH neurons and fibers were visible in the hypothalamic regions (Fig. 7B, Movie 7), as expected. Moreover, we detected robust GnRH immunoreactivity at the caudal end of the OB (Fig. 7C, Movie 7), at the border with the cortex. These GnRH neurons maintained their ring-like distribution around the trunk of the OB (Fig. 7D, Movie 8). Within the OB, GnRH neurons were abundantly distributed inside the structure specialized in pheromone detection, the AOB (Fig. 7D,E). In the adult mouse OB (n=2, 5-month-old females; Fig. 7F,G), GnRH neurons were still detected in the glomerular layer of the main and accessory OB (Fig. 7F,G) as well as in the olfactory nerve layer (Fig. 7H).

DISCUSSION

The GnRH system is the master regulator of reproductive function in vertebrates, and alterations in GnRH signaling and/or neuronal development impair human reproduction. It is therefore crucial to fully understand the mechanisms regulating the ontogenesis, differentiation and prenatal migration of GnRH neurons from the nose to the brain. Here we have conducted comprehensive anatomical studies of human embryos/fetuses in order to obtain better insight into the development of GnRH neurons during the first trimester of gestation. The unprecedented use of whole-mount immunolabeling and 3DISCO technology coupled with LSM in order to carry out high-resolution visualization of markers for various cell and fiber types in whole embryos/fetuses has led to several novel observations concerning this system that could not have been achieved with conventional histological analysis. These findings open new avenues in the study of human brain connectivity under physiological and pathological conditions. For instance, this study has undertaken the first quantitative analysis of GnRH neurons in human fetuses. We have established that, on average, ~10,000 GnRH-immunoreactive neurons are present in the human brain during fetal development. This number is significantly higher than previously thought. Indeed, using immunohistochemistry, many laboratories have assessed the number and distribution of GnRH neurons in the brains of several mammalian species, with estimates ranging from 800 cells in the entire brain in adult rodents to 2000 neurons in the hypothalamus of adult primates (Crowley et al., 2008; King and Anthony, 1984; Latimer et al., 2000; Silverman et al., 1982; Tobet et al., 2001). It is worth noting that the number of GnRH neurons in mice is higher during embryonic development (1000-1200 neurons) and declines at adulthood (Messina et al., 2011; Parkash et al., 2012). This might not be the case in humans, where *GNRH1* mRNA-expressing cells remain widespread in hypothalamic as well as extrahypothalamic regions (Rance et al., 1994). Of note, Rance and colleagues extended the analysis of the distribution of GnRH cells by *in situ* hybridization to several areas of the adult human brain (Rance et al., 1994) and reported a similar number of neurons to our findings during fetal development. However, there has been a certain degree of skepticism until now as to whether the extrahypothalamic population would eventually also produce a mature GNRH1 peptide. Our data now reinforce that study and suggest that the entire population of fetal GnRH neurons is likely to survive until adulthood, with negligible cell loss. Moreover, the similar anatomical distribution of GnRH cells in human fetuses and in adult brains suggests that, by the end of the first trimester of gestation, GnRH cells occupy their final brain location, with ~2000 neurons located in the hypothalamus and ~8000 neurons distributed in widespread brain areas that are not involved in the control of the hypothalamic-pituitary-gonadal axis.

It has previously been shown in other species that GnRH-expressing neurons migrate into the brain along branches of the VNN and TN (Schwanzel-Fukuda and Pfaff, 1989; Wray et al., 1989), both of which emerge from the vomeronasal epithelium and run medially from the olfactory epithelium towards the dorsal region of the OB. However, their central entry point differs: the VNN reaches the AOB, whereas the TN projects ventrally and dorsally within the forebrain to target septal, hypothalamic and limbic areas (Pearson, 1941a; Schwanzel-Fukuda and Silverman, 1980; Wirsig-Wiechmann and Oka, 2002; Wray et al., 1989) involved in controlling innate behaviors and neuroendocrine responses. Whether GnRH neurons in humans also reach their target areas using this axonal scaffold was unknown until now. Using whole-mount immunolabeling and 3DISCO, we found that GnRH neurons migrate into several hypothalamic and extrahypothalamic brain regions in tight association with peripherin-positive VNN/TN fibers. This indicates that the vomeronasal and terminal systems play important roles in the ontogenesis and migration of GnRH neurons in humans, similar to other mammals. This raises the possibility that some genetic forms of congenital hypogonadotropic hypogonadism in humans, characterized by GnRH deficiency and the failure of puberty onset, might be due to defective central projections of the TN, causing insufficient/aberrant GnRH migration. In agreement with this hypothesis, previous studies have shown that intracranial projections of the VNN/TN, which express neuropilin 1 (NRP1), the receptor for the guidance molecule semaphorin 3A, fail to enter the brain and instead accumulate at the dorsal surface of the cribriform plate in mice lacking a functional semaphorin-binding domain in NRP1 ($Nrp1^{sema/sema}$ mice) (Hanchate et al., 2012) or semaphorin 3A ($Sema3a^{-/-}$ mice) (Cariboni et al., 2011). Concordantly, deficient semaphorin 3A signaling appears to contribute to some human genetic reproductive disorders characterized by defective GnRH migration, such as Kallmann syndrome (Hanchate et al., 2012; Young et al., 2012).

Another striking finding is the existence of an evolutionarily conserved dorsal migratory path for GnRH neurons within the brain.

Development (2016) 143, 3969-3981 doi:10.1242/dev.139444

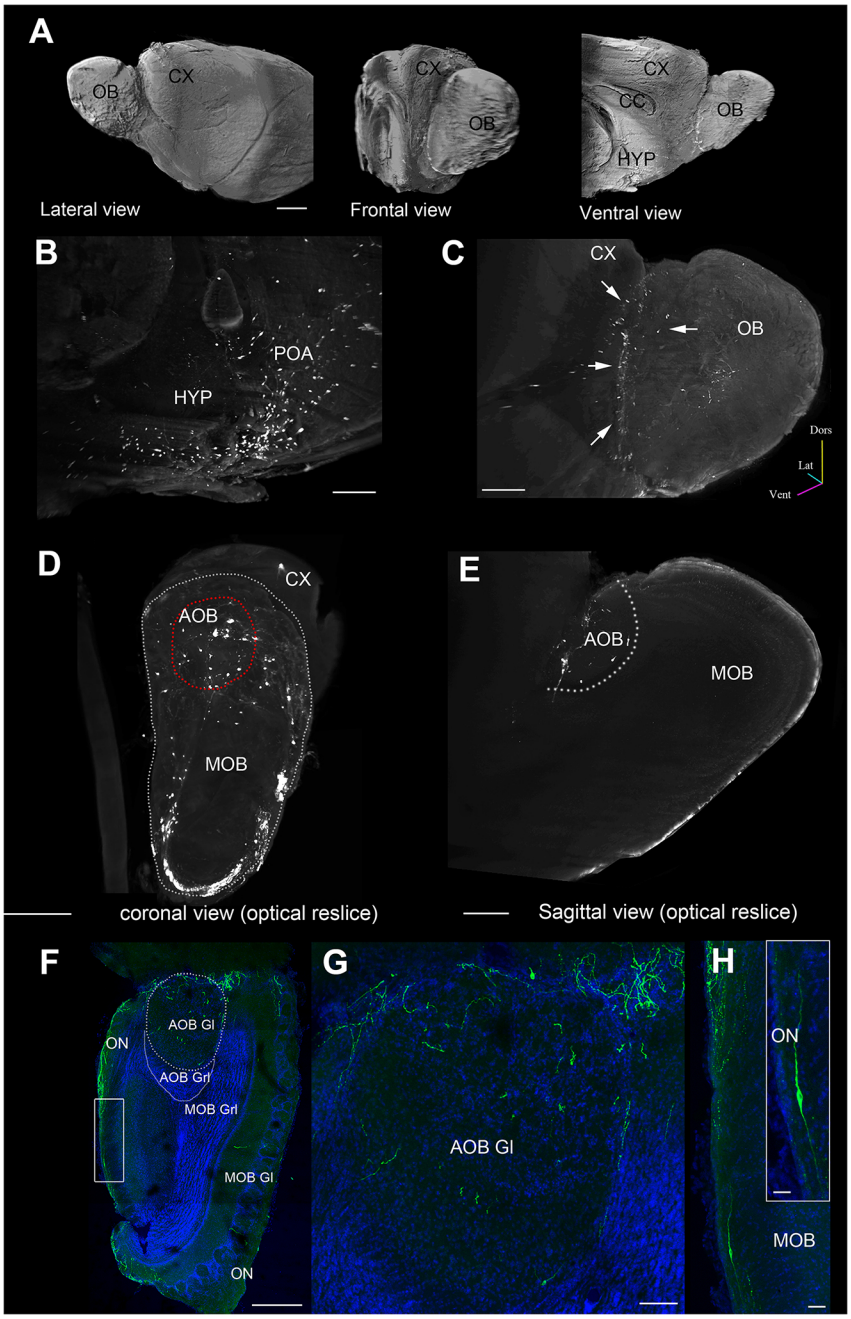

Fig. 7. Whole-mount immunolabeling and 3DISCO clearing of adult mouse brain hemispheres. (A-E) Adult mouse brain hemisphere immunolabeled for GnRH (4-month-old males, *n*=2). (A) Lateral, frontal and ventral views after digital surface contrast masks. (B,C) Lateral views of the entire transparent hemi-brain showing GnRH neurons in the preoptic-hypothalamic regions (B) and in the OB (C, arrows). (D,E) Rostral and sagittal optical sections of the OB containing GnRH neurons. (F-H) GnRH immunoreactivity in a representative coronal section of an adult mouse OB (5-month-old-females, *n*=2). (F) Low-magnification confocal photomicrograph of the OB showing the distribution of GnRH cells and fibers in the glomerular layer (Gl) of the main olfactory bulb (MOB) and accessory olfactory bulb (AOB), and in the olfactory nerve layer (ON). (G,H) High-magnification photomicrograph of the AOB (G) and ON (H). CC, corpus callosum; Grl, granular layer; POA, preoptic area; other abbreviations as previous figures. Scale bars: A, 1 mm; B, 400 µm; C, 700 µm; D, 500 µm; E, 300 µm; F, 120 µm; G, 30 µm; H, 20 µm; inset in H, 10 µm.

A similar observation was made in non-human primates 20 years ago (Quanbeck et al., 1997), but was not confirmed or extended to any other species. In the present study we identified GnRH neurons along the two migratory streams in both human and mouse embryos, and both species possessed unexpected GnRH neuronal populations in the NCX and the developing piriform cortex, which is involved in olfaction. An additional previously unreported observation in both species was the presence of a single-cell-thick ring of GnRH neurons around each OB. The topography of these cells bears striking resemblance to a group of olfactory glomeruli called the ‘necklace’ glomeruli, which surround the caudal end of the OBs (Shinoda et al., 1989). The necklace glomeruli have been implicated in detecting pheromones (Lin et al., 2004; Teicher et al., 1980), and our study shows that a significant number of GnRH neurons and fibers are still present during adulthood in the mouse OB and the AOB. This suggests that there might be some as yet undetermined connective or functional link between the GnRH neurons in this structure and neurons involved in olfactory and/or pheromonal discrimination.

A structural and functional link between GnRH neuronal ontogenesis and pheromone detection could also come from our observations concerning the VNO. In humans and other mammals, odors constitute chemosensory cues in the establishment of early interactions between mothers and infants (Dulac et al., 2014), and several studies have identified behavioral responses to pheromonal compounds (Dulac and Torello, 2003). However, the issue of whether these responses are mediated by a functional VNO in humans has been a matter of extensive debate. Previous studies have demonstrated the existence of a distinguishable VNO in a substantial proportion of adult humans (Frasnelli et al., 2011). However, the neuronal connection between the VNO and the AOB has remained elusive. Here, we show that during human fetal

Development (2016) 143, 3969-3981 doi:10.1242/dev.139444

development the VNO and the AOB are indeed anatomically connected, since NRP2-immunoreactive vomeronasal fibers project to the dorsal OB, as reported in rodents (Cloutier et al., 2002). The VNO also contains strongly Ki67-positive and SOX2-positive putative neurogenic precursors, in agreement with the increase in volume of the human fetal VNO epithelium with age and its persistence at least until birth (Bhatnagar and Smith, 2001; Smith and Bhatnagar, 2000).

Finally, the computer-assisted 3D reconstruction of tissue sections immunolabeled for GnRH has allowed the generation of the first 3D atlas of GnRH cell bodies and fibers from GW 9 and GW 12 human fetuses. These mapping experiments have revealed the wide distribution of GnRH cells and terminals in several extrahypothalamic regions. These observations raise the intriguing possibility that GnRH signals to GnRH receptor-expressing neuronal populations dispersed in several brain regions (Granger et al., 2004; Wilson et al., 2006) to modulate as yet unexplored non-reproductive functions, such as the recently proposed regulation of systemic aging (Zhang et al., 2013). Notably, in addition to the extensive GnRH fiber distribution in those areas, GnRH is also present in the cerebrospinal fluid at concentrations proportional to those detected in the portal blood vessels (Van Vugt et al., 1985) and might thus represent an additional source of GnRH that could potentially signal to multiple brain regions.

This study will pave the way for new discoveries concerning the role of GnRH expression and release in human reproductive physiology, olfactory behavior and cognitive processes.

MATERIALS AND METHODS

Tissue collection and processing

The human gestational period spans the embryonic (first 8 weeks) and fetal stages of development. The 23 Carnegie stages cover mostly the embryonic period (~60 days) and provide a standardized system to characterize developmental age based on the internal and external morphology of the human embryo. The ages of the embryos were estimated based on the following criteria: (1) the attending physicians' information about the 'menstrual weeks' age of the embryos, generally 2 weeks greater than the 'postovulatory age'; (2) external morphology of the embryo; (3) embryonic (crown-rump) length. The last two criteria were evaluated using Bayer and Altman's human brain atlas during the late first trimester (Bayer and Altman, 2006) and Bossy's study on the development of olfactory structures in human embryos (Bossy, 1980).

Embryos and fetuses were fixed by immersion in 4% paraformaldehyde (PFA) at 4°C overnight or for 2-5 days depending on sample size. The tissues were cryoprotected in 30% sucrose/PBS at 4°C overnight, embedded in Tissue-Tek OCT compound (Sakura Finetek), frozen in dry ice and stored at −80°C until sectioning. Frozen samples were cut serially at 20 µm using a Leica CM 3050S cryostat (Leica Biosystems). For whole-mount staining and 3DISCO clearing, samples were washed in ice-cold PBS and fixed by immersion in 4% PFA at 4°C for 24 h for GW 6-8 embryos, 3 days for 9 GW fetuses, and 5 days for GW 10-12 fetuses. After fixation, samples were stored at 4°C in 0.1 M PBS pH 7.4 containing 0.01% sodium azide until use.

The number of embryos/fetuses analyzed, the crown-rump length of these specimens and the type of processing are listed in the Table S1.

Immunolabeling

Human tissues were cryosectioned at 20 µm thickness. Immunohistochemistry for GnRH was performed as previously reported (Hanchate et al., 2012). For immunolabeling of mouse tissues (genotyped and tissue prepared as described in the supplementary Materials and Methods), two antibodies previously characterized on mouse sections were used: rabbit anti-GnRH (1:3000), a gift from Prof. G. Tramu (Centre Nationale de la Recherche Scientifique, URA 339, Université Bordeaux I, Talence, France) (Beauvillain and Tramu, 1980); and rabbit anti-GnRH (LR5; 1:1000), a gift from Dr R. Benoit (Montreal General Hospital, Quebec, Canada). Human samples were immunolabeled using a guinea-pig anti-GnRH (EH#1018; 1:10,000), produced by Dr Erik Hrabovszky (Laboratory of Endocrine Neurobiology, Institute of Experimental Medicine of the Hungarian Academy of Sciences, Budapest, Hungary) and previously characterized in post-mortem human hypothalami (Hrabovszky et al., 2011). The mouse antibody directed against the human GnRH-associated peptide 1 (GAP1) was characterized on adult human hypothalami by Skrapits et al. (2015). All primary and secondary antibodies used are listed in Tables S2 and S3.

Incubation in a cocktail of primary antibodies (single, double or triple labeled) diluted in PBS containing 5% normal donkey serum (D9663, Sigma) and 0.3% Triton X-100 (Sigma) for 48 h at 4°C was followed by a cocktail of fluorochrome-conjugated secondary antibodies (all raised in donkey; see Table S3 for details) diluted to 1:500 in PBS for 1-2 h at room temperature.

The number and the distribution of GnRH neurons in fetal brains were analyzed as indicated in the supplementary Materials and Methods.

In situ hybridization

In situ hybridization on sections of CS19 embryos was carried out using a digoxigenin-labeled *GNRH1* cRNA as described in the supplementary Materials and Methods.

Image analysis

For 3D reconstruction, a 9 GW and a 12 GW fetus were serially sectioned in the sagittal plane (20 µm thick), immunolabeled with a GnRH antibody (EH#1018) and counterstained with Hoechst 33342 (1:10,000; Thermo Fisher Scientific, #H3570). A subset of these sections, representing an entire hemisphere of the head, were manually traced with Neurolucida 7.0 (MBF Bioscience) and aligned using Reconstruct software (Fiala, 2005) version 1.1. The nasal region of the GW 9 fetus was sampled using a greater number of sections (mean distance between sections of 140 µm) than the caudal part of the brain (mean distance between sections of 430 µm). For the GW 12 fetus, all sections were spaced 480 µm apart. 3D models were rendered using Blender 2.7 (www.blender.org).

Optical clearing for human fetuses

The 3DISCO optical clearing procedure has been described previously (Belle et al., 2014; Ertürk et al., 2012) and was employed here for human embryos aged 7-8 GW. Pre-methanol treatment was performed to clear the samples of blood clots, as described in the iDISCO protocol (Renier et al., 2014) on 9 GW or older samples, and in adult mouse brains.

Imaging

3D imaging was performed as previously described (Belle et al., 2014). An ultramicroscope (LaVision BioTec) using InspectorPro software (LaVision BioTec) was used for imaging. The step size between successive images was fixed at 2 µm.

3D imaging and image processing

Images, 3D volumes and movies were generated using Imaris ×64 software (version 7.6.1, Bitplane). Stack images were first converted to Imaris files (.ims) using ImarisFileConverter and 3D reconstruction was performed using 'volume rendering'. Optical slices of samples were obtained using the 'orthoslicer' tool. The surface of the samples was created using the 'surface' tool by creating a mask around each volume. 3D pictures and movies were generated using the 'snapshot' and 'animation' tools.

Ethics

Non-pathological human embryos/fetuses were obtained from voluntarily terminated pregnancies with the parent's written informed consent (Gynecology Department, Jeanne de Flandre Hospital, Lille, France). Tissues were made available in accordance with French bylaws (Good Practice Concerning the Conservation, Transformation and Transportation of Human Tissue to be Used Therapeutically, published on December 29, 1998). Permission to use non-pathological human fetal tissues was obtained from the French Agency for Biomedical Research (Agence de la Biomédecine, Saint-Denis la Plaine, France, protocol no. PFS16-002).

Development (2016) 143, 3969-3981 doi:10.1242/dev.139444

Animal studies were approved by the Institutional Ethics Committee for the Care and Use of Experimental Animals of the University of Lille 2 (France). All experiments were performed in accordance with the guidelines for animal use specified by the European Union Council Directive of September 22, 2010 (2010/63/EU).

Acknowledgements
We thank the midwives of the Gynecology Department, Jeanne de Flandre Hospital of Lille (Centre d'Orthogénie), France, for their kind assistance and support; Meryem Tardivel (Imaging Core Facility, SFR-DN2M), Delphine Taillieu and Julien Devassine (University of Lille, Inserm, Animal Core Facility).

Competing interests
The authors declare no competing or financial interests.

Author contributions
F. Casoni was involved in the experimental design, research and preparation of the manuscript and figures. S.A.M. performed 3DISCO experiments and was involved in the preparation of the figures. M.B. performed the 3D imaging with LSM. F.L. performed the 3D reconstruction analysis. C.A. performed the *in situ* hybridization experiments. F. Collier, E.H., S.R., V.P. and A.C. were involved in the interpretation of results and preparation of the manuscript. P.G. designed the study and wrote the paper.

Funding
This work was supported by the Institut National de la Santé et de la Recherche Médicale (INSERM), France [grant number U1172]; Agence Nationale de la Recherche (ANR), France [ANR-14-CE12-0015-01 RoSes and GnRH to P.G.]; and the Fondation pour la Recherche Médicale [DEQ20130326524 to V.P. and DEQ20120323700 to A.C.].

Data availability
Movies are available at the Dryad digital repository (Casoni et al., 2016): http://dx.doi.org/10.5061/dryad.7v928.

Supplementary information
Supplementary information available online at
http://dev.biologists.org/lookup/doi/10.1242/dev.139444.supplemental

References
Abraham, E., Palevitch, O., Gothilf, Y. and Zohar, Y. (2009). The zebrafish as a model system for forebrain GnRH neuronal development. *Gen. Comp. Endocrinol.* **164**, 151-160.

Barraud, P., St John, J. A., Stolt, C. C., Wegner, M. and Baker, C. V. H. (2013). Olfactory ensheathing glia are required for embryonic olfactory axon targeting and the migration of gonadotropin-releasing hormone neurons. *Biol. Open* **2**, 750-759.

Bayer, S. A. and Altman, J. (2006). The human brain during the late first trimester. In *Atlas of Human Nervous System Development*, Vol. 4, pp. 1-8. Boca Raton, FL: Taylor & Francis.

Beauvillain, J. C. and Tramu, G. (1980). Immunocytochemical demonstration of LH-RH, somatostatin, and ACTH-like peptide in osmium-postfixed, resin-embedded median eminence. *J. Histochem. Cytochem.* **28**, 1014-1017.

Belle, M., Godefroy, D., Dominici, C., Heitz-Marchaland, C., Zelina, P., Hellal, F., Bradke, F. and Chédotal, A. (2014). A simple method for 3D analysis of immunolabeled axonal tracts in a transparent nervous system. *Cell Rep.* **9**, 1191-1201.

Bhatnagar, K. P. and Smith, T. D. (2001). The human vomeronasal organ. III. Postnatal development from infancy to the ninth decade. *J. Anat.* **199**, 289-302.

Boehm, U., Bouloux, P. M., Dattani, M. T., de Roux, N., Dodé, C., Dunkel, L., Dwyer, A. A., Giacobini, P., Hardelin, J. P., Juul, A. et al. (2015). Expert consensus document: European Consensus Statement on congenital hypogonadotropic hypogonadism-pathogenesis, diagnosis and treatment. *Nat. Rev. Endocrinol.* **11**, 547-564.

Bond, C. T., Hayflick, J. S., Seeburg, P. H. and Adelman, J. P. (1989). The rat gonadotropin-releasing hormone: SH locus: structure and hypothalamic expression. *Mol. Endocrinol.* **3**, 1257-1262.

Bossy, J. (1980). Development of olfactory and related structures in staged human embryos. *Anat. Embryol.* **161**, 225-236.

Brown, J. W. (1987). The nervus terminalis in insectivorous bat embryos and notes on its presence during human ontogeny. *Ann. N. Y. Acad. Sci.* **519**, 184-200.

Bruneau, G., Izvolskaia, M., Ugrumov, M., Tillet, Y. and Duittoz, A. H. (2003). Prolonged neurogenesis during early development of gonadotropin-releasing hormone neurones in sheep (Ovis Aries): in vivo and in vitro studies. *Neuroendocrinology* **77**, 177-186.

Cariboni, A., Hickok, J., Rakic, S., Andrews, W., Maggi, R., Tischkau, S. and Parnavelas, J. G. (2007). Neuropilins and their ligands are important in the migration of gonadotropin-releasing hormone neurons. *J. Neurosci.* **27**, 2387-2395.

Cariboni, A., Davidson, K., Rakic, S., Maggi, R., Parnavelas, J. G. and Ruhrberg, C. (2011). Defective gonadotropin-releasing hormone neuron migration in mice lacking SEMA3A signalling through NRP1 and NRP2: implications for the aetiology of hypogonadotropic hypogonadism. *Hum. Mol. Genet.* **20**, 336-344.

Casoni, F., Malone, S. A., Belle, M., Luzzati, F., Collier, F., Allet, C., Hrabovszky, E., Rasika, S., Prevot, V., Chedotal, A. and Giacobini, P. (2016). Data from: Development of the neurons controlling fertility in humans: new insights from 3D imaging and transparent fetal brains. *Dryad Digital Repository*. doi:10.5061/dryad.7v928.

Christian, C. A. and Moenter, S. M. (2010). The neurobiology of preovulatory and estradiol-induced gonadotropin-releasing hormone surges. *Endocr. Rev.* **31**, 544-577.

Cloutier, J.-F., Giger, R. J., Koentges, G., Dulac, C., Kolodkin, A. L. and Ginty, D. D. (2002). Neuropilin-2 mediates axonal fasciculation, zonal segregation, but not axonal convergence, of primary accessory olfactory neurons. *Neuron* **33**, 877-892.

Crowley, W. F., Jr., Pitteloud, N. and Seminara, S. (2008). New genes controlling human reproduction and how you find them. *Trans. Am. Clin. Climatol. Assoc.* **119**, 29-37.

Dulac, C. and Torello, A. T. (2003). Sensory systems: molecular detection of pheromone signals in mammals: from genes to behaviour. *Nat. Rev. Neurosci.* **4**, 551-562.

Dulac, C., O'Connell, L. A. and Wu, Z. (2014). Neural control of maternal and paternal behaviors. *Science* **345**, 765-770.

Eiraku, M., Hirata, Y., Takeshima, H., Hirano, T. and Kengaku, M. (2002). Delta/notch-like epidermal growth factor (EGF)-related receptor, a novel EGF-like repeat-containing protein targeted to dendrites of developing and adult central nervous system neurons. *J. Biol. Chem.* **277**, 25400-25407.

Ertürk, A. and Bradke, F. (2013). High-resolution imaging of entire organs by 3-dimensional imaging of solvent cleared organs (3DISCO). *Exp. Neurol.* **242**, 57-64.

Ertürk, A., Becker, K., Jährling, N., Mauch, C. P., Hojer, C. D., Egen, J. G., Hellal, F., Bradke, F., Sheng, M. and Dodt, H.-U. (2012). Three-dimensional imaging of solvent-cleared organs using 3DISCO. *Nat. Protoc.* **7**, 1983-1995.

Fiala, J. C. (2005). Reconstruct: a free editor for serial section microscopy. *J. Microscopy* **218**, 52-61.

Forni, P. E., Taylor-Burds, C., Melvin, V. S., Williams, T. and Wray, S. (2011). Neural crest and ectodermal cells intermix in the nasal placode to give rise to GnRH-1 neurons, sensory neurons, and olfactory ensheathing cells. *J. Neurosci.* **31**, 6915-6927.

Frasnelli, J., Lundström, J. N., Boyle, J. A., Katsarkas, A. and Jones-Gotman, M. (2011). The vomeronasal organ is not involved in the perception of endogenous odors. *Hum. Brain Mapp.* **32**, 450-460.

Fueshko, S. and Wray, S. (1994). LHRH cells migrate on peripherin fibers in embryonic olfactory explant cultures: an in vitro model for neurophilic neuronal migration. *Dev. Biol.* **166**, 331-348.

Giacobini, P., Messina, A., Morello, F., Ferraris, N., Corso, S., Penachioni, J., Giordano, S., Tamagnone, L. and Fasolo, A. (2008). Semaphorin 4D regulates gonadotropin hormone–releasing hormone-1 neuronal migration through PlexinB1–Met complex. *J. Cell Biol.* **183**, 555-566.

Gleeson, J. G., Lin, P. T., Flanagan, L. A. and Walsh, C. A. (1999). Doublecortin is a microtubule-associated protein and is expressed widely by migrating neurons. *Neuron* **23**, 257-271.

Gorham, J. D., Baker, H., Kegler, D. and Ziff, E. B. (1990). The expression of the neuronal intermediate filament protein peripherin in the rat embryo. *Dev. Brain Res.* **57**, 235-248.

Gorham, J. D., Ziff, E. B. and Baker, H. (1991). Differential spatial and temporal expression of two type III intermediate filament proteins in olfactory receptor neurons. *Neuron* **7**, 485-497.

Granger, A., Ngô-Muller, V., Bleux, C., Guigon, C., Pincas, H., Magre, S., Daegelen, D., Tixier-Vidal, A., Counis, R. and Laverrière, J.-N. (2004). The promoter of the rat gonadotropin-releasing hormone receptor gene directs the expression of the human placental alkaline phosphatase reporter gene in gonadotrope cells in the anterior pituitary gland as well as in multiple extrapituitary tissues. *Endocrinology* **145**, 983-993.

Guillemin, R. (1967). The adenohypophysis and its hypothalamic control. *Annu. Rev. Physiol.* **29**, 313-348.

Hanchate, N. K., Giacobini, P., Lhuillier, P., Parkash, J., Espy, C., Fouveaut, C., Leroy, C., Baron, S., Campagne, C., Vanacker, C. et al. (2012). SEMA3A, a gene involved in axonal pathfinding, is mutated in patients with Kallmann syndrome. *PLoS Genet.* **8**, e1002896.

Hrabovszky, E., Molnár, C. S., Sipos, M. T., Vida, B., Ciofi, P., Borsay, B. A., Sarkadi, L., Herczeg, L., Bloom, S. R., Ghatei, M. A. et al. (2011). Sexual dimorphism of kisspeptin and neurokinin B immunoreactive neurons in the infundibular nucleus of aged men and women. *Front. Endocrinol.* **2**, 80.

Kim, K. H., Patel, L., Tobet, S. A., King, J. C., Rubin, B. S. and Stopa, E. G. (1999). Gonadotropin-releasing hormone immunoreactivity in the adult and fetal human olfactory system. *Brain Res.* **826**, 220-229.

Development (2016) 143, 3969-3981 doi:10.1242/dev.139444

King, J. C. and Anthony, E. L. P. (1984). LHRH neurons and their projections in humans and other mammals: species comparisons. *Peptides* **5** Suppl. 1, 195-207.
Latimer, V. S., Rodrigues, S. M., Garyfallou, V. T., Kohama, S. G., White, R. B., Fernald, R. D. and Urbanski, H. F. (2000). Two molecular forms of gonadotropin-releasing hormone (GnRH-I and GnRH-II) are expressed by two separate populations of cells in the rhesus macaque hypothalamus. *Mol. Brain Res.* **75**, 287-292.
Lin, W., Arellano, J., Slotnick, B. and Restrepo, D. (2004). Odors detected by mice deficient in cyclic nucleotide-gated channel subunit A2 stimulate the main olfactory system. *J. Neurosci.* **24**, 3703-3710.
Luzzati, F., Fasolo, A. and Peretto, P. (2011). Combining confocal laser scanning microscopy with serial section reconstruction in the study of adult neurogenesis. *Front. Neurosci.* **5**, 70.
Messina, A., Ferraris, N., Wray, S., Cagnoni, G., Donohue, D. E., Casoni, F., Kramer, P. R., Derijck, A. A., Adolfs, Y., Fasolo, A. et al. (2011). Dysregulation of Semaphorin7A/beta1-integrin signaling leads to defective GnRH-1 cell migration, abnormal gonadal development and altered fertility. *Hum. Mol. Genet.* **20**, 4759-4774.
Miller, A. M., Treloar, H. B. and Greer, C. A. (2010). Composition of the migratory mass during development of the olfactory nerve. *J. Comp. Neurol.* **518**, 4825-4841.
Miyamoto, K., Hasegawa, Y., Nomura, M., Igarashi, M., Kangawa, K. and Matsuo, H. (1984). Identification of the second gonadotropin-releasing hormone in chicken hypothalamus: evidence that gonadotropin secretion is probably controlled by two distinct gonadotropin-releasing hormones in avian species. *Proc. Natl. Acad. Sci. USA* **81**, 3874-3878.
Muller, F. and O'Rahilly, R. (2004). Olfactory structures in staged human embryos. *Cells Tissues Organs* **178**, 93-116.
Murakami, S. and Arai, Y. (1994). Direct evidence for the migration of LHRH neurons from the nasal region to the forebrain in the chick embryo: a carbocyanine dye analysis. *Neurosci. Res.* **19**, 331-338.
Murakami, S., Kikuyama, S. and Arai, Y. (1992). The origin of the luteinizing hormone-releasing hormone (LHRH) neurons in newts (Cynops pyrrhogaster): the effect of olfactory placode ablation. *Cell Tissue Res.* **269**, 21-27.
Palevitch, O., Kight, K., Abraham, E., Wray, S., Zohar, Y. and Gothilf, Y. (2007). Ontogeny of the GnRH systems in zebrafish brain: in situ hybridization and promoter-reporter expression analyses in intact animals. *Cell Tissue Res.* **327**, 313-322.
Parkash, J., Cimino, I., Ferraris, N., Casoni, F., Wray, S., Cappy, H., Prevot, V. and Giacobini, P. (2012). Suppression of beta1-integrin in gonadotropin-releasing hormone cells disrupts migration and axonal extension resulting in severe reproductive alterations. *J. Neurosci.* **32**, 16992-17002.
Pearson, A. A. (1941a). The development of the nervus terminals in man. *J. Comp. Neurol.* **75**, 39-66.
Pearson, A. A. (1941b). The development of the olfactory nerve in man. *J. Comp. Neurol.* **75**, 199-217.
Quanbeck, C., Sherwood, N. M., Millar, R. P. and Terasawa, E. (1997). Two populations of luteinizing hormone-releasing hormone neurons in the forebrain of the rhesus macaque during embryonic development. *J. Comp. Neurol.* **380**, 293-309.
Quinton, R., Hasan, W., Grant, W., Thrasivoulou, C., Quiney, R. E., Besser, G. M. and Bouloux, P.-M. (1997). Gonadotropin-releasing hormone immunoreactivity in the nasal epithelia of adults with Kallmann's syndrome and isolated hypogonadotropic hypogonadism and in the early midtrimester human fetus. *J. Clin. Endocrinol. Metab.* **82**, 309-314.
Rance, N. E., Young, W. S., III and McMullen, N. T. (1994). Topography of neurons expressing luteinizing hormone-releasing hormone gene transcripts in the human hypothalamus and basal forebrain. *J. Comp. Neurol.* **339**, 573-586.
Renier, N., Wu, Z., Simon, D. J., Yang, J., Ariel, P. and Tessier-Lavigne, M. (2014). iDISCO: a simple, rapid method to immunolabel large tissue samples for volume imaging. *Cell* **159**, 896-910.
Ronnekleiv, O. K. and Resko, J. A. (1990). Ontogeny of gonadotropin-releasing hormone-containing neurons in early fetal development of rhesus macaques. *Endocrinology* **126**, 498-511.
Schwanzel-Fukuda, M. and Pfaff, D. W. (1989). Origin of luteinizing hormone-releasing hormone neurons. *Nature* **338**, 161-164.
Schwanzel-Fukuda, M. and Silverman, A. J. (1980). The nervus terminalis of the guinea pig: a new luteinizing hormone-releasing hormone (LHRH) neuronal system. *J. Comp. Neurol.* **191**, 213-225.
Schwanzel-Fukuda, M., Bick, D. and Pfaff, D. W. (1989). Luteinizing hormone-releasing hormone (LHRH)-expressing cells do not migrate normally in an inherited hypogonadal (Kallmann) syndrome. *Mol. Brain Res.* **6**, 311-326.
Schwanzel-Fukuda, M., Crossin, K. L., Pfaff, D. W., Bouloux, P. M. G., Hardelin, J.-P. and Petit, C. (1996). Migration of luteinizing hormone-releasing hormone (LHRH) neurons in early human embryos. *J. Comp. Neurol.* **366**, 547-557.
Shinoda, K., Shiotani, Y. and Osawa, Y. (1989). "Necklace olfactory glomeruli" form unique components of the rat primary olfactory system. *J. Comp. Neurol.* **284**, 362-373.
Silverman, A. J., Antunes, J. L., Abrams, G. M., Nilaver, G., Thau, R., Robinson, J. A., Ferin, M. and Krey, L. C. (1982). The luteinizing hormone-releasing hormone pathways in rhesus (Macaca mulatta) and pigtailed (Macaca nemestrina) monkeys: new observations on thick, unembedded sections. *J. Comp. Neurol.* **211**, 309-317.
Skrapits, K., Kanti, V., Savanyú, Z., Maurnyi, C., Szenci, O., Horváth, A., Borsay, B. A., Herczeg, L., Liposits, Z. and Hrabovszky, E. (2015). Lateral hypothalamic orexin and melanin-concentrating hormone neurons provide direct input to gonadotropin-releasing hormone neurons in the human. *Front. Cell Neurosci.* **9**, 348.
Smith, T. D. and Bhatnagar, K. P. (2000). The human vomeronasal organ. Part II: prenatal development. *J. Anat.* **197**, 421-436.
Teicher, M. H., Stewart, W. B., Kauer, J. S. and Shepherd, G. M. (1980). Suckling pheromone stimulation of a modified glomerular region in the developing rat olfactory bulb revealed by the 2-deoxyglucose method. *Brain Res.* **194**, 530-535.
Tobet, S. A., Bless, E. P. and Schwarting, G. A. (2001). Developmental aspect of the gonadotropin-releasing hormone system. *Mol. Cell. Endocrinol.* **185**, 173-184.
Valverde, F., Santacana, M. and Heredia, M. (1992). Formation of an olfactory glomerulus: morphological aspects of development and organization. *Neuroscience* **49**, 255-275.
Van Vugt, D. A., Diefenbach, W. D., Alston, E. and Ferin, M. (1985). Gonadotropin-releasing hormone pulses in third ventricular cerebrospinal fluid of ovariectomized rhesus monkeys: correlation with luteinizing hormone pulses. *Endocrinology* **117**, 1550-1558.
Verney, C., Lebrand, C. and Gaspar, P. (2002). Changing distribution of monoaminergic markers in the developing human cerebral cortex with special emphasis on the serotonin transporter. *Anat. Rec.* **267**, 87-93.
Vilensky, J. A. (2014). The neglected cranial nerve: nervus terminalis (cranial nerve N). *Clin. Anat.* **27**, 46-53.
Wilson, A. C., Salamat, M. S., Haasl, R. J., Roche, K. M., Karande, A., Meethal, S. V., Terasawa, E., Bowen, R. L. and Atwood, C. S. (2006). Human neurons express type I GnRH receptor and respond to GnRH I by increasing luteinizing hormone expression. *J. Endocrinol.* **191**, 651-663.
Wirsig-Wiechmann, C. R. and Oka, Y. (2002). The terminal nerve ganglion cells project to the olfactory mucosa in the dwarf gourami. *Neurosci. Res.* **44**, 337-341.
Witkin, J. W., Dao, D., Livne, I., Dunn, I. C., Zhou, X. L., Pula, K. and Silverman, A. J. (2003). Early expression of chicken gonadotropin-releasing hormone-1 in the developing chick. *J. Neuroendocrinol.* **15**, 865-870.
Wray, S., Grant, P. and Gainer, H. (1989). Evidence that cells expressing luteinizing hormone-releasing hormone mRNA in the mouse are derived from progenitor cells in the olfactory placode. *Proc. Natl. Acad. Sci. USA* **86**, 8132-8136.
Wray, S., Key, S., Qualls, R. and Fueshko, S. M. (1994). A subset of peripherin positive olfactory axons delineates the luteinizing hormone releasing hormone neuronal migratory pathway in developing mouse. *Dev. Biol.* **166**, 349-354.
Yoshida, K., Tobet, S. A., Crandall, J. E., Jimenez, T. P. and Schwarting, G. A. (1995). The migration of luteinizing hormone-releasing hormone neurons in the developing rat is associated with a transient, caudal projection of the vomeronasal nerve. *J. Neurosci.* **15**, 7769-7777.
Young, J., Metay, C., Bouligand, J., Tou, B., Francou, B., Maione, L., Tosca, L., Sarfati, J., Brioude, F., Esteva, B. et al. (2012). SEMA3A deletion in a family with Kallmann syndrome validates the role of semaphorin 3A in human puberty and olfactory system development. *Hum. Reprod.* **27**, 1460-1465.
Zhang, G., Li, J., Purkayastha, S., Tang, Y., Zhang, H., Yin, Y., Li, B., Liu, G. and Cai, D. (2013). Hypothalamic programming of systemic ageing involving IKK-beta, NF-kappaB and GnRH. *Nature* **497**, 211-216.

Supplementary methods

Mouse tissue preparation

C57BL/6J mice (Charles River, USA) were housed under specific pathogen-free conditions in a temperature-controlled room (21-22°C) with a 12h light/dark cycle and ad libitum access to food and water. Embryonic day 16.5 (E 16.5) embryos were harvested from timed-pregnant C57BL/6J mice, fixed in 4% PFA overnight at 4°C and stored at 4°C in PBS containing 0.01% sodium azide whole-mount immunolabeling. Adult mice (n = 2, 4 month-old male mice; n = 2, 5 month-old female mouse) were anesthetized with 100 mg/kg of ketamine-HCl and 10 mg/kg xylazine-HCl and perfused transcardially with 4% PFA. Brains were collected, postfixed in the same fixative for 4 h at 4°C, and the two hemispheres of each brain were stored at 4°C in PBS containing 0.01% sodium azide until whole-mount immunolabeling.

GnRH cell counting

Serial coronal sections (20 µm) from embryos and fetuses were cut and labeled for GnRH as described above. Four serial series were generated for CS16 (n = 1), five serial series were generated for CS17-CS19 (CS17-18, n = 3), six series for older embryos and fetuses were generated (CS19-23, n = 3; GW 9-10, n = 5; GW 11-12, n = 3). GnRH-immunolabeled sections were examined using an Axio Imager.Z1 ApoTome microscope (Zeiss, Germany), equipped with a motorized stage and an AxioCam Mrm camera (Zeiss, Germany). To visualize and count the cells a Zeiss 20x objective (N.A. 0.8) was used. GnRH neurons were counted every 80 µm spanning the entire head of embryos and fetuses. Total numbers of GnRH cells were calculated in each sample and combined to give group means ± SEM. All analyses were performed using Prism 5 (GraphPad Software) and assessed for normality (Shapiro-Wilk test) and variance, when appropriate. Sample sizes were chosen according to the standard practice in the field. Data for GnRH cell number between the four groups analyzed (CS17-18, CS19-23, GW 9-10, GW 11-12) were compared by one-way ANOVA followed by Bonferroni's *post hoc* analysis test.

Total numbers of GnRH cells were also calculated as a function of sex in fetuses aged 7-10 GW (n = 4 males; n = 4 females). Data were compared by a two-tailed unpaired Student's t test. In all statistical tests, the significance level was set at $p < 0.05$.

PCR

For genotyping 2 pairs of primers were used for SRY: SRY1 sense 5'-CAGGCCATGCACAGAGAGAA-3' antisense 5'-GGTAAGTGGCCTAGCTGGTG-3' and SRY2 sense 5'-ACGCATTCATCGTGTGGTCT-3' and antisense 5'-AACTGCAATTCTTCGGCAGC-3'

Fluorescent *In Situ* Hybridization (FISH)

Three CS 19 whole embryos were fixed by immersion in 4% PFA at 4°C for 24 h. The sections (16 µm) were cut on a cryostat, mounted on Superfrost Plus slides (Fisher Scientific, Pittsburgh, PA), and stored at –80°C until processing for hybridization. We employed a fluorescence *in situ* hybridization procedure using a digoxigenin-11-UTP (Dig)-labeled GnRH-1 cRNA probe transcribed from a rat GnRH-1 cDNA, previously published (Bond et al., 1989). The riboprobes were synthesized *in vitro* with 1 µg linearized GnRH cDNA, 1X digoxigenin RNA labeling mixture (Roche), RNA polymerase (T7 for antisense and SP6 for sense), and 1X transcription buffer. This mixture was incubated at 37°C (T7)

or at 39°C (SP6) for 2 h. Residual DNA was digested with deoxyribonuclease. The probes (1 µg/µl) were diluted 1:200 with hybridization buffer. Following treatment with proteinase K (5 µg/ml in Tris 0.1M, EDTA 0.05M, DEPC H_2O, pH 8) and acetic anhydride, the sections were incubated for 2 h at room temperature (RT) in prehybridization buffer (50% formamide, sodium chloride–sodium citrate SSC 5X, Denhardt's solution 1 mg/ml, yeast tRNA 250 µg/ml, herrings sperm DNA 500 µg/ml, H_2O DEPC) before being hybridized overnight at 60 °C with Dig-GnRH-1 cRNA. The next day, the slides were washed at high stringency (final wash: 0.2X SSC at 60 °C for 1 h). Thereafter, the sections were incubated for 1 h at RT in blocking buffer containing Tris-HCl 0.1M pH 7.5, NaCl 0.15 M, 0.5% blocking reagent (Roche). Following these blocking steps, the sections were incubated for 45 min at RT with anti-Dig-POD (Roche) diluted in TNT buffer (Tris-HCl 0.1M pH 7.5, NaCl 0.15 M, 0.5% Triton X-100). Then, the sections were washed in TNT buffer (three times, 10 min each) before a 15 min incubation at RT with tyramide signal amplification reagent (TSA)-biotin Stand Alone Tyramide Kit (PerkinElmer) diluted 1:50. Finally, the sections were incubated with Streptavidin 568 (Thermo Fisher Scientific) diluted 1:200 in TNT buffer for 45 min at RT, counterstained with Hoechst 33258 (Termo Fisher Scientific) for 1 min, washed in PBS and coverslipped with aqueous mounting medium before fluorescence microscopic examination.

Supplementary tables

Table S1. List of embryos/fetuses analyzed and experimental paradigm

Stage (CS or GW)	Number of specimens analyzed	Crown rump length (mm)	Experiment
CS 16 (GW 5.5)	1	8	IHC/GnRH cell quantification
CS 17 (GW 6)	2	11-13	IHC/GnRH cell quantification
CS 18 (GW 6)	1	15	IHC/GnRH cell quantification
CS 19 (GW 7)	1	17	IHC/ISH/GnRH cell quantification
CS 23 (GW 8)	2	25-28	IHC/GnRH cell quantification
GW 9	3	29-32	IHC/GnRH cell quantification
GW 10	2	38-40	IHC/GnRH cell quantification
GW 11	2	45-47	IHC/GnRH cell quantification
GW 12	1	50	IHC/GnRH cell quantification
GW 10	1	42	IHC a-hGAP1/a-GnRH
GW 12	1	55	IHC a-hGAP1/a-GnRH
CS 19 (GW 7)	1	18	IHC/3DISCO/LSM
CS 21 (GW 7.5)	1	22	IHC/3DISCO/LSM
GW 9	1	29	IHC/3DISCO/LSM
GW 9	1	31	IHC/iDISCO/LSM
GW 9	2	30	3D Reconstruction
GW 12	2	50-55	3D Reconstruction
Total number	**25**		

A total of 9 human embryos (Carnegie Stage, CS, 16-23) and 16 fetuses (Gestational Week, GW, 9-12) were used in this study. The number of embryos/fetuses analyzed, the crown-rump length of these specimens and the type of experiments are listed in the table. CS 16: approximately 39 days of gestation; CS 17: approximately 41 days of gestation; CS 18: approximately 44 days of gestation; CS 19: approximately 48 days of gestation; CS 21: approximately 53 days of gestation; CS 23: approximately 56 days of gestation. Abbreviations: IHC, immunohistochemistry; ISH, *In situ* hybridization; LSM, light sheet microscopy.

Table S2. List of primary antibodies used for immunofluorescence

Antigen	Host species	Source	Dilution
GnRH	Rabbit	Prof. G. Tramu, University of Bordeaux, France	1:4000
GnRH	Rabbit	LR5, Dr. R. Benoit, Montréal General Hospital, Montréal, Québec, Canada	1:10000
GnRH	Guinea-Pig	Dr. Erik Hrabovszky, Institute of Experimental Medicine of the Hungarian Academy of Sciences, Budapest, Hungary	1:10000
hGAP1	Mouse	Dr. Erik Hrabovszky, Institute of Experimental Medicine of the Hungarian Academy of Sciences, Budapest, Hungary	1:2000
Doublecortin (DCX)	Goat	Santa Cruz, SC-8066	1:500
β-III tubulin (TUJ1)	Mouse	Sigma, T8660	1:800
Delta/notch-like EGF-related receptor (DNER)	Goat	R&D system, AF2254	1:200
PAX6	Rabbit	Millipore, AB2237	1:400
HuC-D	Mouse	Termo Fisher Scientific A21271	1:200
Ki67	Rabbit	Abcam, ab15580	1:200
Peripherin	Rabbit	Millipore, AB1530	1:1000
SOX2	Goat	Santa Cruz, sc-17320	1:300
SOX10	Goat	N-20; Santa Cruz; sc-17342	1:200
AP-2 alpha	Goat	3B5 supernatant 1:3; DSHB	1:200
Transient Axonal Glycoprotein-1 (TAG-1)	Goat	R&D system AF2215	1:500
Neuropilin-2 (NRP-2)	Goat	R&D system AF2215	1:400

Table S3. List of secondary antibodies used for immunofluorescence

Antibody	Host species	Reference	Dilution
Anti-Goat AF®488	Donkey	Termo Fisher Scientific A-11055	1:500
Anti-Goat AF®568	Donkey	Termo Fisher Scientific A- 11057	1:500
Anti-Goat AF®647	Donkey	Termo Fisher Scientific A-21447	1:500
Anti-Rabbit AF®488	Donkey	Termo Fisher Scientific A-21206	1:500
Anti-Rabbit AF®568	Donkey	Termo Fisher Scientific A-10042	1:500
Anti-Rabbit AF®647	Donkey	Jackson IR 706-605-152	1:500
Anti-Mouse AF®488	Donkey	Termo Fisher Scientific A-21202	1:500
Anti-Mouse AF®568	Donkey	Termo Fisher Scientific A-10037	1:500
Anti-Guinea Pig AF®488	Donkey	Jackson IR 706-545-148	1:500
Anti-Guinea Pig AF®594	Donkey	Jackson IR 706-585-148	1:500
Anti-Guinea Pig AF®647	Donkey	Jackson IR 706-605-148	1:500

Supplementary figures

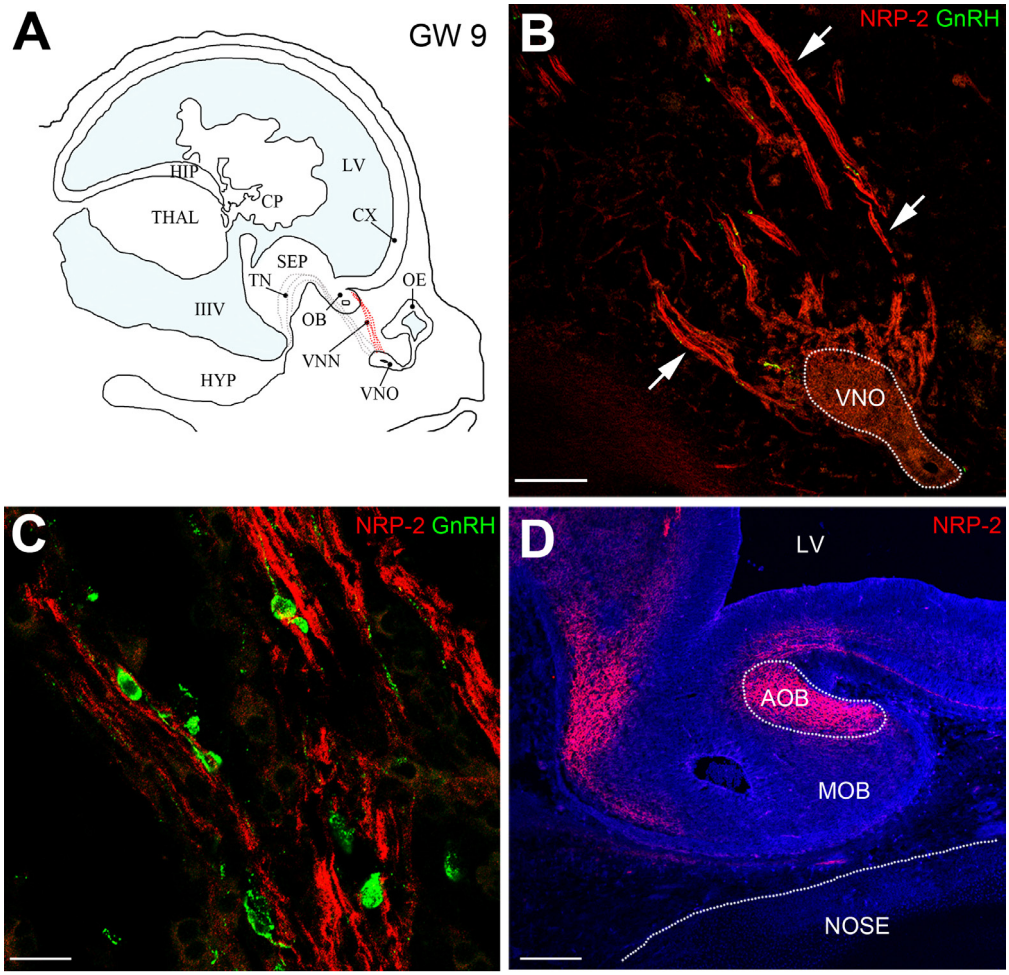

Figure S1. AOB is anatomically connected with VNO. (A) Schematic representation of a sagittal section of a GW 9 head. (B-C) Sagittal sections through the nose of a GW 9 fetus immunolabeled for NRP-2 and GnRH. (B) NRP-2 is expressed by the vomeronasal nerve (VNN; arrows). (C) High power photomicrograph showing GnRH neurons migrating toward the forebrain along the NRP-2-immunoreactive VNN. (D) NRP-2-immunoreactive fibers project to the accessory olfactory bulb (AOB) but not the main olfactory bulb (MOB). VNO: vomeronasal organ; OE: olfactory epithelium; OB: olfactory bulb; SEP: septum; TN: terminal nerve; CX: cortex; LV: lateral ventricle; CP: choroid plexus; HIP: developing dorsal hippocampus; THAL: thalamus; IIIV: third ventricle; HYP: hypothalamus. Scale bars: B, 100 μm; C, 20 μm; D, 80 μm.

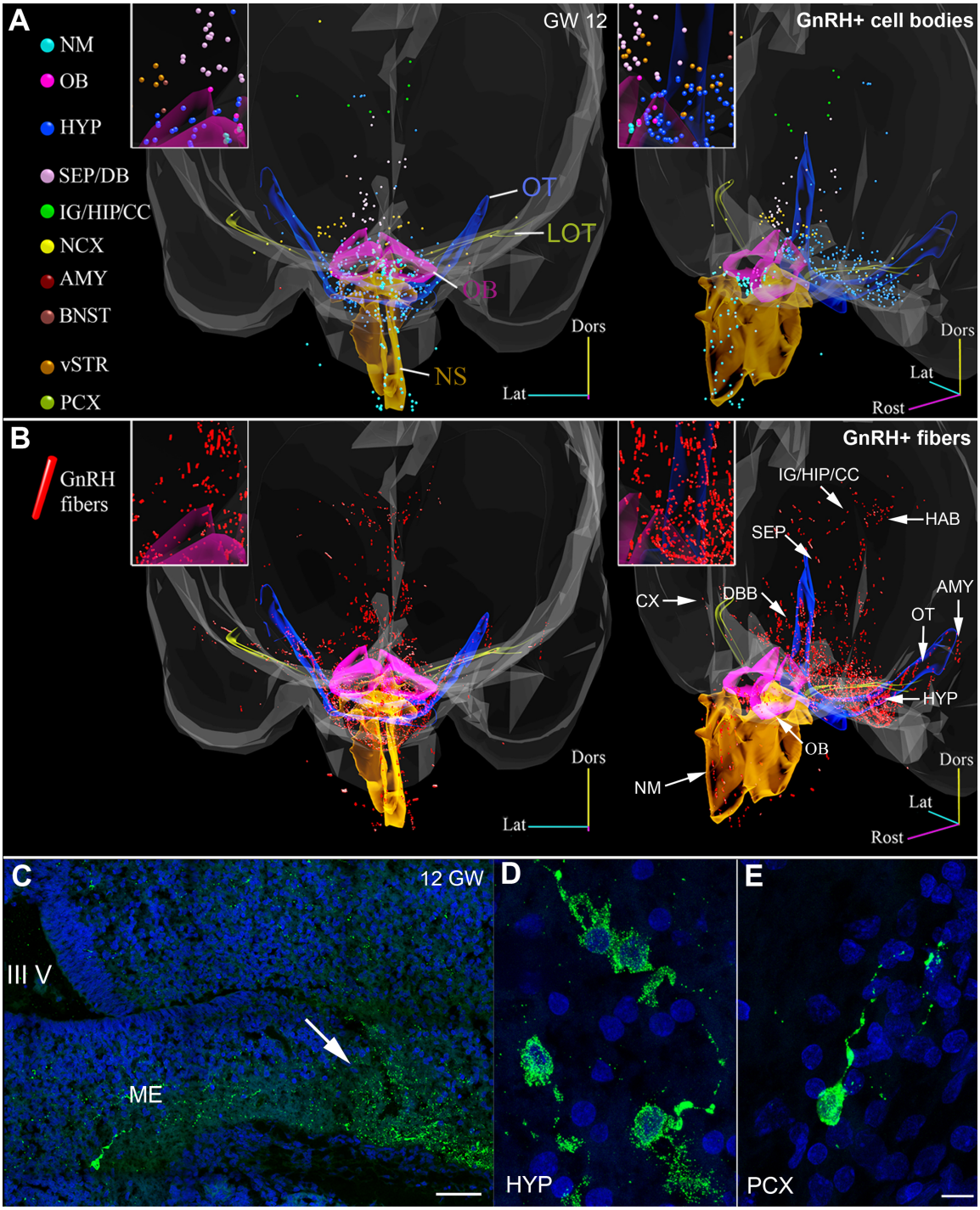

Figure S2. Distribution of GnRH cell bodies and neurites at GW 12. (A) Front (left) and perspective (right) views of a 3D model of GnRH neuronal cell body distribution in a GW 12 embryo. Each cell is represented by a sphere (100 μm in diameter) colored according to its location (see legend on the left). Transparent contours of nasal septum (NS), olfactory bulb (OB), lateral olfactory tract (LOT) and optic tract (OT) are also shown for reference. Higher magnification of a small detail of the 3D model is shown. (B) Same views of the 3D models in A) showing the distribution of GnRH fibers (red bars). (C-E) Representative sections of a GW 12 fetal brain immunolabeled for GnRH. GnRH terminals are already detectable in the median eminence (ME, arrows in C) and GnRH expressing cells are found in the hypothalamus (HYP, D) and piriform cortex (PCX, E). Scale bars: C, 40 μm; D, E, 10 μm.

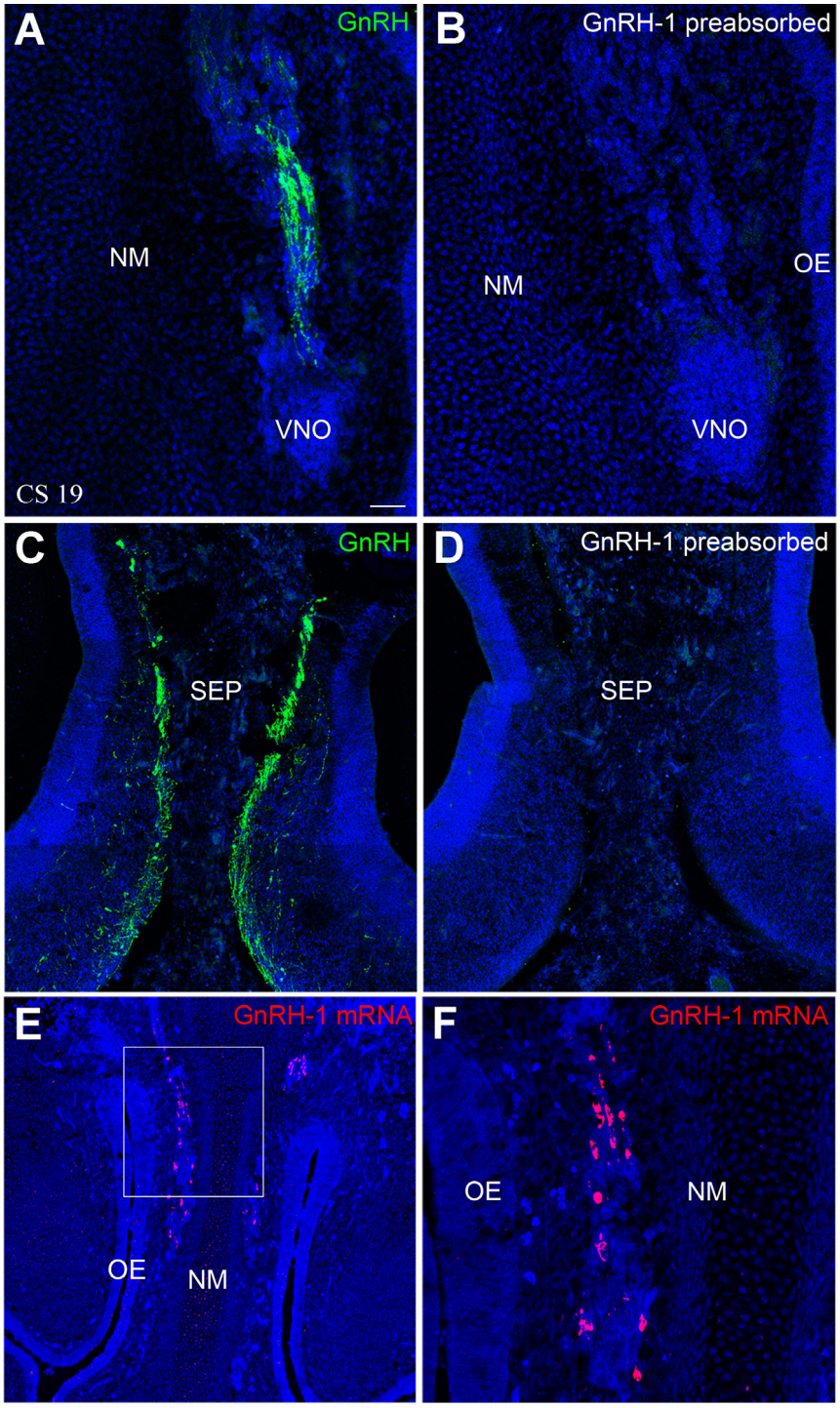

Figure S3. Validation of the specificity of GnRH expression in human embryonic head sections. (A-D) Representative coronal sections of a CS 19 nose (A, B) and forebrain (C, D) immunolabeled for GnRH. (B, D) Adjacent sections of A and C incubated with anti-GnRH antibody preadsorbed with GnRH-1 peptide. (E, F) Representative coronal sections of a CS 19 nose containing migratory neurons expressing GnRH mRNA (marked in red in the figure, fluorescent *in situ* hybridization). The image represented in (F) is a higher magnification of the boxed area in (E). SEP: septum; OE: olfactory epithelium; NM: nasal mesenchyme. Scale bars: A, B, 50 μm; C, D, 100 μm; E, 80 μm; F, 20 μm.

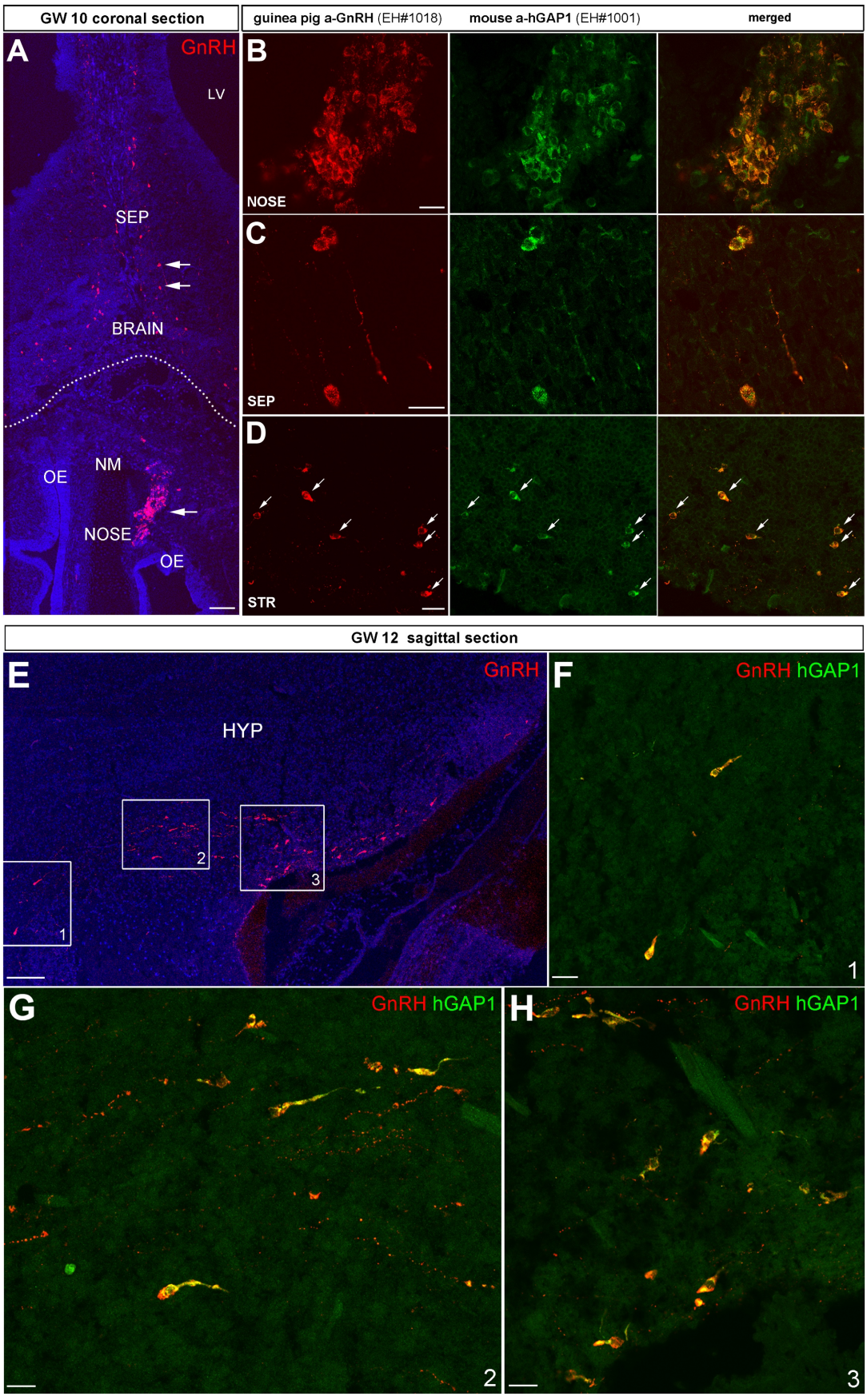

Figure S4. GnRH neurons in human fetal brains express the GnRH-1 form. Representative confocal photomicrographs of coronal sections of a GW 10 head (A-D) and a sagittal section of a GW

12 head (E-H) immunolabeled for GnRH (red) and the human GnRH-associated peptide 1 (GAP1, green). (B and C) are higher magnifications images of cells in A (arrows). There is a complete colocalization of GnRH and GAP1 in neurons distributed across several areas, including the nose (B), the septum (SEP, C) and the striatum (STR, D), as evidenced in the merged images. (F-H) are higher magnifications images of the boxed areas shown in the hypothalamus (HYP, E). The complete colocalization between the two antigens (B-D and F-H) confirms that GnRH-immunoreactive neurons of the human fetal brain contain the GnRH-1 form. NM: nasal mesenchyme; OE: olfactory epithelium. Scale bars: A, 80 μm; B-D, 20 μm; E, 100 μm; F-H 20 μm.